



Open Research Online

The Open University's repository of research publications and other research outputs

Dating martian climate change

Journal Item

How to cite:

Page, David P.; Balme, Matthew R. and Grady, Monica M. (2009). Dating martian climate change. *Icarus*, 203(2) pp. 376–389.

For guidance on citations see [FAQs](#).

© 2009 Elsevier

Version: [\[not recorded\]](#)

Link(s) to article on publisher's website:

<http://dx.doi.org/doi:10.1016/j.icarus.2009.05.012>

Copyright and Moral Rights for the articles on this site are retained by the individual authors and/or other copyright owners. For more information on Open Research Online's data [policy](#) on reuse of materials please consult the policies page.

oro.open.ac.uk

Accepted Manuscript

Dating martian climate change

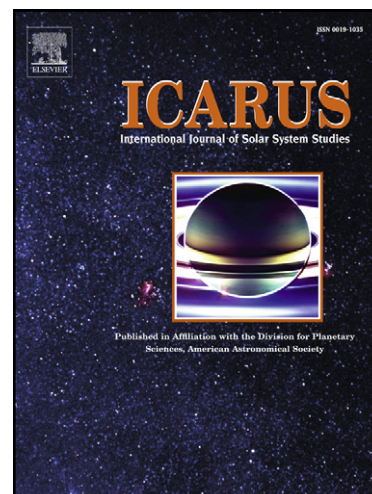
David P. Page, Matthew R. Balme, Monica M. Grady

PII: S0019-1035(09)00228-0
DOI: [10.1016/j.icarus.2009.05.012](https://doi.org/10.1016/j.icarus.2009.05.012)
Reference: YICAR 9048

To appear in: *Icarus*

Received Date: 27 January 2009
Revised Date: 6 May 2009
Accepted Date: 11 May 2009

Please cite this article as: Page, D.P., Balme, M.R., Grady, M.M., Dating martian climate change, *Icarus* (2009), doi: [10.1016/j.icarus.2009.05.012](https://doi.org/10.1016/j.icarus.2009.05.012)



This is a PDF file of an unedited manuscript that has been accepted for publication. As a service to our customers we are providing this early version of the manuscript. The manuscript will undergo copyediting, typesetting, and review of the resulting proof before it is published in its final form. Please note that during the production process errors may be discovered which could affect the content, and all legal disclaimers that apply to the journal pertain.

Dating Martian Climate Change

David P. Page¹, Matthew R. Balme^{2,3}, Monica M. Grady^{1,4}

¹Planetary and Space Sciences Research Institute,
The Open University,
Milton Keynes MK7 6AA.
U.K.
D.P.Page@open.ac.uk

²Department of Earth and Environmental Sciences
The Open University
Milton Keynes MK7 6AA.
U.K.

³Also at: The Planetary Science Institute
1700 E. Fort Lowell
Suite 106
Tucson
AZ 85719
USA

⁴Also at: Dept. of Mineralogy
Natural History Museum
Cromwell Rd.
London SW7 5BD

Running head: Dating Martian Climate Change

Address editorial correspondence and proofs to:

David Page

Planetary and Space Science Research Institute,

The Open University, Milton Keynes, MK7 6AA.

Telephone: (US) 202 248 2497

Email: D.P.Page@open.ac.uk

ACCEPTED MANUSCRIPT

Abstract

Geological evidence indicates that low-latitude polygonally-patterned grounds on Mars, generally thought to be the product of flood volcanism, are periglacial in nature and record a complex signal of changing climate. By studying the martian surface stratigraphically (in terms of the geometrical relations between surface landforms and the substrate) rather than genetically (by form analogy with Earth), we have identified dynamic surfaces across one fifth of martian longitude. New stratigraphical observations in the Elysium-Amazonis plains have revealed a progressive surface polygonisation that is destructive of impact craters across the region. This activity is comparable to the climatically-driven degradation of periglacial landscapes on Earth, but because it affects impact craters – the martian chronometer – it can be dated. Here we show that it is possible to directly date this activity based on the fraction of impact craters affected by polygon formation. Nearly 100% of craters (of all diameters) are superposed by polygonal sculpture: considering the few-100 Ma age of the substrate, this suggests that the process of polygon formation was active within the last few million years. Surface polygonisation in this region, often considered to be one of the signs of young, 'plains-forming' volcanism on Mars, is instead shown to postdate the majority of impact craters seen. We therefore conclude that it is post-depositional in origin and an artifact of thermal cycling of near-surface ground ice. Stratigraphically-controlled crater counts present the first way of dating climate change on a planet other than Earth: a record that may tell us something about climate change on our own planet. Parallel climate change on these two worlds – an ice age Mars coincident with Earth's glacial Quaternary period – might suggest a coupled system linking both. We have previously been unable to generalise about the causes of long-term climate change based on a single terrestrial example – with the beginnings of a chronology for climate change on our nearest planetary neighbour, we can.

27 Introduction

28 A recurrent theme in studies of martian climate change is its recency: gullies, 'frozen oceans',
29 sorted patterned-ground and a host of other glacial-periglacial (cold-climate) landforms attest to the
30 relative youth of climatic events on Mars. However, the most spatially extensive of these landforms
31 have impact crater densities consistent with surface ages of 10s to a few 100 million years (Ma), incon-
32 sistent with a youthful, climatic origin [McEwen et al., 2005]. New observations of polygonally-patterned
33 grounds in the Elysium-Amazonis plains (Figs. 1-2) overturn this notion of great age, revealing that cra-
34 ter counts are not telling the whole story, an anomaly that has its origins in the general volcanic theory
35 of how these regions were formed. While some aspects of surface morphology in this area are sugges-
36 tive of volcanism [Keszthelyi et al., 2000; Plescia, 2003], the landforms within these deposits display
37 superposition relations with impact craters that indicate regional-scale surface reorganisation at a time
38 far-removed from deposition [Page and Murray, 2006; Page, 2007, 2008]. Fig. 2a shows a typical ex-
39 ample, in which the polygonal surface sculpture cross-cuts the entire impact crater population, reaching
40 over rim crests and into crater floors (detail inset). Hence this sculpture formed *after* the craters, and a
41 crater count that tells us about the age of the substrate tells us nothing about the age of polygonisation.

42
43 A schematic cross-section can help to visualise this impact-cratered surface structurally. The
44 stylised sections in Fig. 3 show a generalised 'layer cake' stratigraphy (3a) and a polygonised surface of
45 the form seen in the Amazonis plain (3b). The crater in 3a records the age of Unit X, not Unit Y (Unit Y
46 of a thickness insufficient to bury the crater of unit X, which stands proud of the upper unit as a result).
47 However, this is not what is going on in Fig. 3b, or in the Amazonis plain. What appears on first inspec-
48 tion of Fig. 2a to be a polygonal surface covered in impact craters is actually an impact-cratered surface
49 covered in polygons. This distinction is more than semantic, for it means that a standard crater count
50 does not capture the true age of this polygonal surface at all (a geometry with consequences for the
51 lithology of the substrate). The crater in Fig. 3b records the age of the substrate, Unit X, but *not* the age
52 of polygonisation (which postdates the crater). This polygonal sculpture also occurs within erosional

53 drainage channels (Fig. 4), a further sign of secondary origin illustrating the generality of these observa-
54 tions (see Appendix A1). The volcanic theory, based on visual similarities to terrestrial lava flow sur-
55 faces, interprets the superposing polygonal and conical landforms in these deposits as cooling and ex-
56 plosive features coeval with the substrate [Keszthelyi et al., 2000; Jaeger et al., 2007]. In contrast, ge-
57 ology shows these to be dynamic, time-transgressive (or diachronous) surfaces whose age is decou-
58 pled from the substrate. As such, current estimates of surface age derived from crater counts [e.g.,
59 Hartmann and Berman, 2000; Hartmann and Neukum, 2001; Plescia, 2003] must be reconsidered.

60
61 Aspects of the morphology and chronology of the deposits of the late Amazonian-aged (300-600
62 Ma to present [Hartmann and Neukum, 2001]) Elysium-Amazonis plains have been considered else-
63 where [Plescia, 2003; Jaeger et al., 2007; Hartmann and Neukum, 2001; Burr et al., 2002]. Here we
64 focus on near-surface structure, as expressed through stratigraphical superposition, demonstrating that
65 these surfaces have been active in the very recent past, and assert that this modification is an indicator
66 of climatic change. Further, we speculate on a link between the timing of climate change on Mars and
67 the drivers of long-term terrestrial climate change.

68 69 **Geochronology**

70 As an exogenic event, impact cratering is post-depositional by definition; therefore, any landform
71 that crosses a crater rim must itself be post-depositional, and postdate impact (see Appendix A1-A2).
72 Because impact craters are the means of estimating surface age on Mars, any constructive process
73 that affects impact craters in large numbers can be dated, the proportion of craters affected, relative to
74 total counts, providing a measure of the recency (if not inception) of the process in question.

75
76 It is customary in impact crater chronology for inferences regarding geological events to be
77 drawn from trends in crater size-frequency distribution (SFD) based on counts of the total number of
78 impact craters in a given area, e.g., flattening of the SFD can be an indication of erosional loss of cra-

79 ters [Hartmann, 2005], while an increase in the slope of the SFD may suggest exhumation of a previ-
80 ously buried surface [Malin et al., 2006]. Here we invert this logic and count craters in the polygonal
81 ground based on superposition relationships. This allows us to divide the SFD into stratigraphically-
82 (hence, temporally-) distinct sub-populations depending on whether impact craters are observed to pre-
83 or post-date formation of the polygonal sculpture (see Appendix A1). In Fig. 2a, all the visible impact
84 craters are transected by this surface sculpture, thus it is reasonable to infer that the polygonisation of
85 the substrate is substantially younger than its deposition. To quantify this age of polygonisation, we un-
86 dertook a crater counting study of polygonally-patterned grounds across the Elysium-Amazonis region.

87

88 The counts were performed using full-resolution HiRISE images (25 cm / pixel) on platy and po-
89 lygonally-patterned ground at five locations, covering an area of $\sim 60 \text{ km}^2$ at the eastern and western
90 limits of the Cerberus Formation (Tables 1-2). We counted all features that could be reliably interpreted
91 as of impact origin (see Appendix A3), defining three sub-populations of impact craters: 'Group 1' cra-
92 ters that predate polygonisation (i.e., where polygons reach the crater rim), 'Group 2' craters that post-
93 date polygonisation (i.e., where ejecta embays polygons), and 'Group 3' craters for which no strati-
94 graphical determination can be made (i.e., those that are sufficiently small to avoid intersection with the
95 polygonal sculpture, and therefore may either pre- or post-date the sculpture as a result (e.g., Fig. A1c).
96 Because the temporal affinities of Group 3 craters are unclear, we have deliberately included them with
97 the "postdate" count (Group 2) to avoid any bias toward a younger age for polygonisation. Thus, we ob-
98 tained two ages for each area: i) the emplacement age of the substrate (all craters counted), and ii) the
99 oldest age for polygonal sculpture formation (Group 2). Results are given in Fig. 2 and Tables 1-2.

100

101 Fig. 2b shows the crater SFD for the area of polygonal terrain in Fig. 2a, alongside a 'control'
102 count of craters in a neighbouring, less-polygonised area. Most of the craters in the polygonal areas ($>$
103 98%; $> \sim 10 \text{ m}$ diameter) predate formation of the polygonal sculpture (i.e., are in Group 1). For diame-
104 ters between $\sim 40 \text{ m}$ and 500 m , the SFDs follow the isochrons midway between 100 Ma and 1 Ga,

105 consistent with reported surface ages of a few-100 Ma [e.g., Hartmann and Neukum, 2001; Burr et al.,
106 2002]. Below 40 m, the SFD in the polygonal areas (Fig. 2b, red plot, middle) flattens dramatically, mov-
107 ing below the 100 Ma isochron to cross the 10 Ma and 1 Ma isochrons, a trend maintained down to the
108 smallest measured diameters (~ 4 m). This flattening increases with increasing polygonisation, those
109 craters in less polygonised areas (Fig. 2b, black plot, right) clearly describing a steeper path. The near-
110 horizontal section of the plot ($D \sim 6$ m and below) is an artefact of decreasing image resolution, but the
111 roll-over beginning at 40 m cannot be so attributed. At 25 cm / pixel, a 40 m crater is 160 pixels across
112 and perfectly visible – it is not possible in a HiRISE image for non-detection of craters to be a function
113 of image resolution at this diameter. We attribute the roll-over to the destructive effects of polygon for-
114 mation (see Fig. 2a inset and Appendix A1).

115

116 The small fraction of impact craters that postdate polygon formation (Group 2, Fig. 2b, blue plot,
117 left) describe a path between the 100 ka and 1 Ma isochrons, with a single outlier between 1 Ma and 10
118 Ma (arrowed). There is cause to regard this few-Ma age-range as robust: the largest Group 2 crater ob-
119 served (Fig. 4b) is 90 m in diameter, a size consistent with a surface age of < 10 Ma for the ~ 60 km²
120 area counted [Hartmann and Neukum, 2001]. Together, these three stratigraphical groups of impact
121 craters ('predate', 'postdate', and 'indeterminate') constrain polygon formation to within the last 5 Ma.

122

123 We tested our hypothesis of a dynamic, recently active surface in Amazonis Planitia in the
124 source region and type area for these deposits: Athabasca Valles, in Elysium Planitia. It has previously
125 been observed that there are consistent age differences between different parts of individual flow sur-
126 faces in this region, the polygonal surfaces measurably younger than the 'platy' ground to which they
127 are interstitial [Murray et al., 2005]. The age difference is reported to be slight, on the order of 10⁵
128 years, and within the statistical errors of the crater counts. However, using new HiRISE observations
129 (Fig. 2c-e), we have found the age difference to be substantial, closer to 100 Ma, with the polygonal
130 regions far younger. The time-gap is unambiguous, the bulk of the craters concentrated in the platy re-

131 gions (Figs. 2c, 2e) with the SFD in platy and polygonal areas plotting along ~ 100 Ma and 5 Ma
132 isochrons respectively (Fig. 2d). This age-difference varies considerably throughout the region, but its
133 expression here is telling. Such evidence requires that either one surface is younger than the other, or
134 something is removing craters in the polygonal areas. It is unlikely that any process – including poly-
135 gonisation – could obscure or obliterate ~ 100 Ma of craters in the inter-plate areas whilst leaving those
136 on nearby plates intact, so the polygonal ground must be younger, supporting a late-stage, secondary
137 origin for polygon formation across the Elysium-Amazonis plains.

138

139 The temporal discontinuity between these two surface morphologies is impossible to reconcile
140 with either a single surface of solid rock [e.g., Plescia, 2003; Keszthelyi et al., 2000] or an emplacement
141 duration of "...a few to several weeks" [Jaeger et al., 2008a]. Instead, it is most likely that these deposits
142 are the sedimentary remnant of outflow channel formation [Rice et al., 2002] or the residuum of a once-
143 greater ice mass [e.g., Murray et al., 2005], reworked periglacially over time [Page, 2007]. The visual
144 impression is that the surfaces in Figs. 2c and 2e accumulated the bulk of their craters before break-up,
145 that plate fracture and movement, like polygonal ground formation, are also recent events. This qualita-
146 tive impression is confirmed by the measured difference in crater density between platy and polygonal
147 surfaces – Table 2 showing over 95% of the craters in Fig. 2e concentrated in the plates, relative to the
148 polygonal ground. For any given crater diameter in the most numerous and statistically-reliable diame-
149 ter bins ($D = \sim 8\text{-}22$ m), crater density is 10-20x greater in the platy regions than the polygonal. Craters
150 counted in the polygonal inter-plate regions of Fig. 2e were in the 6-30 m diameter range, at which size
151 the craters have rim heights of ~ 0.5-2 m. The lesser of these values provides an index of the maximum
152 dust thickness for the craters counted to be visible, so dust infill cannot account for the local 10-fold dif-
153 ference in impact crater density between these two surfaces across the observed diameter range.

154

155 Given the disparity in surface ages between these two surface morphologies, it is notable that
156 the pitted mounds characteristic of these deposits (Fig. 2e, centre; also 3c-d and 4b-f) occupy both

157 platy and polygonal regions and hence must postdate both [e.g., Page and Murray, 2006; Page, 2008;
158 cf. Jaeger et al., 2007, 2008b]. Their presence within platy ground removes any possibility that these
159 are rocky materials surrounded by later, polygonally-patterned effluvium [e.g., Burr and Parker, 2006].
160 This dynamic, discordant surface is consistent with indications of ongoing mound growth, the 'wakes'
161 formed downstream of the older mounds in Fig. 2e clearly severed where the plates have rafted apart
162 (white arrows), with new post-fracture mounds forming over the breach (dark arrows [cf. Figs. 4g-h]).
163 The geological history of this surface may be delineated on the basis of these relative age-relations
164 (Table 3), a story of continuous change over many millions of years.

165

166 This large time gap (or disconformity) helps answer one question regarding the timing of surface
167 change in Fig. 2a. Although we can constrain the recency of polygonisation, it is not possible to say
168 from the superposition of impact craters in Amazonis Planitia when the process of polygon formation
169 began (i.e., whether this is a wholly young phenomenon that postdates the majority of impact craters
170 here, or if it has been active throughout the 100s of millions of years recorded by these craters, the lat-
171 est phase of activity polygonising those craters last formed). Given the ubiquity of this surface sculpture
172 across this region (and in deposits of a range of ages throughout the northern lowlands generally), it is
173 probable that what is seen in Fig. 2a is a complex, compound signal rather than a discrete event. Nev-
174 ertheless, the similarity in the ages of polygonisation in Amazonis Planitia (Fig. 2a-b) and Athabasca
175 Valles (Fig. 2d-e) suggests that events across Elysium-Amazonis may indeed be entirely young.

176

177 To put all of these observations into context, we must recognise that there are two ages re-
178 corded in the surface of Fig. 2a: a substrate age documented by the total number of impact craters, and
179 a secondary age of 'overprint', independent of any assertion of process, that records a later phase of
180 endogenic activity (see Appendix A1-A2). There is only one process on Earth that results in decametre-
181 scale post-depositional polygon formation – thermal cycling of near-surface volatiles [French, 1996] –
182 and it is this that we believe has produced polygonisation of the deposits of the martian equator.

183 **Land form and Climate**

184 We suggest that the young overprint of craters is climatic in origin, a periglacial hypothesis
185 based on form and association of surface landforms long-noted in the deposits of this region [Rice et
186 al., 2002], but previously debarred on the basis of apparent great surface age [McEwen et al., 2005]. As
187 the most widespread feature the polygonal surface sculpture is the landform most amenable to dating,
188 but this is just one part of an assemblage of landforms of putative periglacial origin that exist in these
189 deposits (Fig. 4c-f), each with its parallel in the terrestrial cold-climate environment and the same sec-
190 ondary relation to the substrate [Page, 2007, 2008; Balme et al., 2009]. This assemblage includes po-
191 lygonal ground, pingo-like (or ice-cored) mounds, thermokarst-like subsidence pits (a feature related to
192 ground ice loss), solifluction ridges (the product of thaw-induced surface creep) and sorted stone cir-
193 cles, a mixture of constructional and degradational landforms collectively diagnostic of freeze-thaw ac-
194 tivity on Earth and, in association, unique to permafrozen terrain [Dylik, 1964; Washburn, 1980; French,
195 1996]. While such landform interpretations are rarely definitive in planetary imaging, where different
196 causes or processes may result in strikingly similar visual effects [Schumm, 1991; Page and Murray,
197 2006], such convergence of form is the rationale for the approach from which our chronology derives, a
198 geomorphology grounded in geological structure that is both a test of hypotheses and a guard against
199 the deceptions of resemblance that beset all planetary image interpretation [Zimbelman, 2001].

200

201 The climatic implications of this landform assemblage are well recognised on Earth and equated
202 with periods of intense cold during the last glacial maximum, ~ 15 kyr ago [Washburn, 1980]. Terrestrial
203 permafrost exists today far south of the 0°C isotherm where it is in disequilibrium with present climate
204 and actively degrading, such ground-ice thought to be relict of former, colder climes before Pleistocene
205 deglaciation [Péwé, 1983; Osterkamp and Burn, 2002]. We suggest that the periglacial landscape seen
206 across the Elysium-Amazonis plains today has a similar disequilibrium origin, occurring just where it
207 should if formed by climatic changes within the last few Ma, i.e., at the warmest latitudes on the planet
208 (during northern hemisphere summer). Because the spatial extent of permafrost generally changes with

209 climate [Washburn, 1980; Osterkamp and Burn, 2002], and climate is the only process known to be lati-
210 tude-dependent [Head et al., 2003], the low-latitude distribution of this assemblage serves as a test of
211 climatic control. At the current orbital inclination (25° [Fig. 6]), near-surface ground-ice is stable only at
212 high latitude (poleward of $\sim 60^\circ$ [Mellon and Jakosky, 1995]), becoming progressively less stable to-
213 ward the equator; a model assertion confirmed spectrally [Boynton et al., 2002]. The corollary is that it
214 is in the zone of *lowest* ground ice stability that the *youngest* signs of periglacial activity should be most
215 apparent. Because the orbital axis of Mars, like Earth's, is not fixed, this zone of instability shifts with
216 changing obliquity, residing at high latitude at high tilt and low latitude at low tilt (the current condition).
217 As orbital inclination has moved from a state of high mean obliquity to one of low mean obliquity over
218 the last 5 Ma (Fig. 6), ground ice in the tropics will have become increasingly unstable, responding to
219 the elevated surface temperature by cycling of near-surface volatiles. The colder conditions in this re-
220 gion before 5 Ma would have been conducive to periglacial landform genesis, the warming trend since
221 then equally suited to their degradation. The young polygon > thermokarst > pingo sequence is consis-
222 tent with this progressively ameliorating climate, and the presence of comparable but older landforms at
223 higher latitudes [e.g., Siebert and Kargel, 2001; Costard and Kargel, 1995; Farrand and Gaddis, 2003].

224

225 All the features discussed are presumptive evidence of permafrost, based on post-depositional
226 origin and analogy with presently active terrestrial forms [Washburn, 1980]. On Earth, polygonal ground
227 underlain by ice wedges can cease cracking during warmer climatic periods, or lie dormant for long pe-
228 riods of time only to reactivate with renewed cooling. Because the polygonal sculpture in the Elysium-
229 Amazonis plains cross-cuts craters of every diameter (hence age), this precludes these being fossil
230 periglacial polygonal fractures which, when filled with clastic material, can be preserved for hundreds of
231 millions of years on Earth [e.g., Deynoux, 1982].

232

233 So is the young landform assemblage on Mars an indicator of a former, palaeo-climate, or is it a
234 sign of contemporary climate change? We can consider this question by reference to the intrusive

235 mound landforms. Most are degraded (Figs. 5b-d), but many are not (Figs. 5f-h, 2e and Appendix A1d)
236 and are considered to indicate geologically-recent hydrological cycling [Page and Murray, 2006]. While
237 the landforms of this assemblage can only be dated to within the last few Ma, we know that 'pingos' are
238 transient, hydrological features that do not survive over geological time scales (the terrestrial pingo life
239 cycle is ~ 10 kyr [French, 1996]), so it is likely that these martian landforms are very recent features
240 given the visual indications of ongoing mound growth in Fig. 2e. Given the precedent for lagged ground
241 ice decay in the terrestrial environment [Osterkamp and Burn, 2002], it is possible that a delayed re-
242 sponse to recent climate changes is still triggering ground ice activity on Mars today [e.g., Cabrol and
243 Grin, 2002], a possibility supported by ground-penetrating radar data (see Appendix A4).

244

245 Such recency is consistent with models of atmospheric deposition of ground ice on Mars driven
246 by periodic (10^5 yr) variations in the planet's spin axis [Mellon and Jakosky, 1995; Mischna et al., 2003].
247 However, a more direct source of ice is the substrate itself, the channels in which these landforms oc-
248 cur being the site of catastrophic water release in the geologically-recent past. The outflow channels of
249 the Elysium-Amazonis plains – Athabasca and Marte Valles – were undoubtedly cut by running water
250 [Rice et al., 2002; Burr et al., 2002; Burr and Parker, 2006], so evidence exists for recent aqueous ac-
251 tivity and a viable source of volatiles within the region. The question of the origin of this assemblage
252 then becomes one of the preservation of these volatiles, a consideration based on models of ground ice
253 stability, the simplifying geological assumptions of which reflect our lack of knowledge regarding the
254 textural and compositional heterogeneity of the martian regolith [e.g., Clifford, 1998; Chamberlin and
255 Boynton, 2007; Mellon et al., 2004]. The instability of ground ice is often given for the absence of icy
256 landforms at low latitude [e.g., Levrard et al., 2004; Chamberlin and Boynton, 2007], but far from pre-
257 cluding the existence of such a landscape, this instability is the key to its presence. That we do not
258 generally make this connection has more to do with the association of surfaces in this region with flood
259 volcanism than any inability of these latitudes to support ground ice activity on the observed time scales
260 [e.g., Smoluchowski, 1968; Mischna et al., 2003].

261 **Mars and Earth**

262 Assuming that our chronology is correct (see Appendix A2), our observations show that perigla-
263 cial activity occurred on Mars at the same time as the last major period of glaciation on Earth (~ 6 Ma to
264 10 ka [Hays et al., 1976; Eyles, 1993]). This overlap might simply be coincidental: it is accepted that
265 climate changes with orbital modulation, and the orbital geometries of both Earth and Mars vary on a
266 similar 10^4 - 10^5 year timescale*. Alternatively, the parallel climate changes might indicate the action of
267 a single external control, such as solar variability [Sagan and Young, 1973]. Our derived chronology of
268 surface change (~ 5 Ma) is orders of magnitude less exact than the 10^4 - 10^5 yr periods of Mars' orbital
269 variation, so there is no way to confirm or discount either prospect at present. Notwithstanding the pos-
270 sibility that parallel climate change on Mars and Earth is a coincidence of timing rather than cause, we
271 explore the implications for both planets of synchronous climate variations.

272

273 It is accepted that the primary driving force for Quaternary climate change is a seasonal change
274 in insolation induced by variations in Earth's orbital parameters – the 'pacemaker' of the ice ages [Emil-
275 iani, 1955; Hays et al., 1976]. However, no single element of obliquity, precession or orbital eccentricity
276 accounts for the 100-ka cyclicity that dominates the post-Quaternary sedimentary record, or the infre-
277 quency of terrestrial glaciation before this time [Hays et al., 1976; Eyles, 1993; Riall, 1999]. A complex
278 relationship between insolation and mantle-derived CO_2 is therefore thought to provide the primary link
279 with climate through the greenhouse effect, reinforced by the changing distribution of the continents and
280 their influence upon atmospheric and oceanic circulations [e.g., Veevers, 1990; Broeker and Denton,
281 1989; Harris, 2002]. How these various endogenous factors interact, and whether they serve to amplify
282 the effect of the orbital rhythms within Earth's climate system, or vice versa, is unclear [Ruddiman et al.,

283

284

285 *We do not relate surface change on Mars to any particular episode of orbital variation (whose 10^4 - 10^5 -yr periods are beyond constraint by
286 impact crater chronology), the last 5 Ma encompassing ~ 250 precessional and 125 obliquity cycles with frequencies of 21 ka and 41 ka re-
287 spectively. Similarly, while this young periglaciation appears related to recent climatic change it does not presuppose orbital variation as the
288 mechanism of volatile emplacement. Reworking of subsurface ice in this region is inevitable, whether its emplacement is the product of orbital
289 forcing or the happenstance of a catastrophic outflow event, both solutions consistent with the current disposition of ice at low martian latitude.

290 1986], but Mars is a planet that lacks for oceans and plate tectonics (at least on the few-Ma time scale
291 in question [Zuber, 2001]), and one that has a very different atmosphere to our own. Detecting the signs
292 of orbital forcing in earlier Earth epochs is hampered by our inability to constrain short-order events
293 ($\sim 10^5$ yrs time scale) in the terrestrial rock record [Miall and Miall, 2004]. Thus our recognition of events
294 triggered by orbital variations is based on a single, well-dated instance of change over the last ~ 2 Ma
295 (the last terrestrial ice age). In this context the timing of periglaciation on Mars might tell us something
296 about Earth, suggesting that when considering the causes that tip these two planets between green-
297 house and icehouse states, external forcings may have had a greater influence on *long-term* terrestrial
298 climate than previously suspected [e.g., Muller and MacDonald, 1997; Forte and Mitrovica, 1997; Harris,
299 2002].

300

301 We note that there is no reason to suppose that 'ice ages' on Mars should be the same as those
302 on Earth; indeed, it has been suggested that they are opposite in some respects, with martian glacial
303 periods characterised by warmer polar climates (a result of Mars' more extreme obliquity variation) that
304 drive volatiles down to cooler, lower latitudes to be deposited as ice [Head et al., 2003]. Martian 'glacial'
305 periods occur at times of high obliquity ($> \sim 30^\circ$, the last period some 2-0.4 Ma ago) and 'interglacials'
306 at low obliquity (\sim past few 100 ka to the present), when the lower latitudes are warmer and volatile-loss
307 cycles volatiles back to the pole.

308

309 This interpretation, based on a conceptual model of orbitally-forced ground ice emplacement,
310 places Mars in an interglacial period defined by the current low orbital obliquity, the volatile-rich glacial
311 deposits formed at mid-latitude during the previous high-obliquity phase now undergoing reworking,
312 degradation and retreat in response to the present instability of near-surface ground ice [Mustard et al.,
313 2001]. This mechanism does not differ fundamentally from that of Earth, where obliquity-driven varia-
314 tions in insolation at high northern-latitudes are thought to control the growth of the polar ice sheets
315 around whose margins and newly exposed forelands periglacial landform assemblages predominate.

316 This martian 'ice age' hypothesis postulates periglacial activity at a latitude where volatiles are known to
317 exist from spectroscopic observations [Boynton et al., 2002; Feldman et al., 2004], unlike the lower-
318 latitude Elysium-Amazonis plains, where little ground ice is evident from spectrometry data. Neverthe-
319 less, a case exists for suggesting that the degraded periglacial landscape seen in Elysium-Amazonis is
320 just where it should be under current climatic conditions, that young deposits at low latitude should be
321 more strongly reworked, and their periglacial landform assemblage better developed, relative to those
322 at mid-latitude. Most models of atmosphere-regolith volatile exchange on Mars envisage stable ground
323 ice in the tropics during periods of high obliquity [e.g., Mellon and Jakosky, 1995; Mischna et al., 2003;
324 Levrard et al., 2004], the obliquities at which such stability is predicted to occur ($\sim 30^\circ$) achieved as re-
325 cently as 500 ka (Fig. 6). Irrespective of the mechanism of ground-ice emplacement on Mars, if insola-
326 tion is the key to its loss then the most recent degradation should be evident at low-latitude.

327

328 This is indeed the case, with the most diverse assemblage of young periglacial landforms – po-
329 lygonally-sculpted ground, intrusive frost mounds (or 'pingos'), thermokarst, solifluction ridges, and most
330 recently, sorted stone circles and nets – found at low latitude [Page and Murray, 2006; Page, 2007,
331 2008; Balme et al., 2009]. The other classic permafrost feature commonly part of this assemblage is the
332 rock glacier. Although not part of this study, examples of such landforms are widely recognised in the
333 amphitheatres of the Tharsis Montes, directly east of the study area [e.g., Head and Marchant, 2003],
334 these deposits of comparable (late Amazonian) age to those we have observed in the plains.

335

336 A young periglacial landscape at low martian-latitude raises several questions. 1) Are Mars and
337 Earth bound in their response to external forcings? Clearly, orbital variation alone does not predestine
338 climate change; if this were the case, alternating glacial-interglacial periods would have become a regu-
339 lar fixture of Earth history, rather than the handful of times that continent-scale 'icehouse' conditions
340 have obtained during the past three billion years [Eyles, 1993]. Alternatively, orbital forcing might play a
341 dominant role in global climate change, the lack of evidence for more frequent glaciation an artefact of

342 a fragmentary geological record. 2) Is periglaciation at low martian-latitude a response to deglaciation of
343 the northern plains, the buried ice present at higher latitude of ice sheet origin? On the one hand, this
344 ice is located where thermal models suggest it would form if deposited during periods of higher obliquity
345 [Mellon and Jakosky, 1995]. On the other hand, the ice content (~ 70% [Boynton et al., 2002]) is so high
346 that diffusive deposition of water vapour in regolith pore space cannot be the primary formation mecha-
347 nism [Richardson et al., 2003]. 3) Are the high water-vapour and methane fluxes recently observed over
348 the low-latitudes related to ongoing permafrost degradation, a lagged response to an earlier episode of
349 climate change, or even climate change today? Our revised geology of the Elysium region reduces the
350 possibility that serpentinisation of basalt could be the source of this methane (indeed, where are the
351 vast quantities of liquid water required for such regional-scale hydrothermal alteration?). On Earth, such
352 regional concentrations of atmospheric methane are characteristic of ongoing permafrost degradation,
353 with all that this implies for the potential biogenicity of the carbon [e.g., Liblik et al., 1997; Page, 2007].

354

355 We are only just scratching the surface of what Mars may tell us about long-term climate change
356 on Earth – the longest-standing puzzle in Earth science [Raymo and Huybers, 2008]. Using the geo-
357 logical record as a criterion against which to judge the performance of physical and numerical models of
358 chronology and climate [Miall and Miall, 2004; Imbrie and Imbrie, 1980], with two planets on which to
359 explore this puzzle we should have a better chance of solving it than if our investigations were limited to
360 only one [Baker, 2003].

361

362 **Conclusion**

363 An alternative, periglacial interpretation of Mars' equatorial plains, long-suspected on geomor-
364 phological grounds, is corroborated geologically. This interpretation finds agreement in impact crater
365 populations, both relatively, in terms of local disparities in surface crater density, and measurably, in
366 terms of derived Ma-scale surface ages. This recently-active Mars parallels Earth in both the expres-
367 sion and the timing of its surface changes – and perhaps also in its cause.

368 **Acknowledgments**

369 The authors thank Greg Michael of FUB for assistance with the Craterstats program. We would
370 also like to thank Stephanie Werner and an anonymous second reviewer for critical comments that im-
371 proved the manuscript. This research was funded by grants from CEPSAR to DPP and from STFC to
372 MMG and MRB.

373

374

375

376

377

378

379

380

381

382

383

384

385

386

387

388

389

390

391

392

ACCEPTED MANUSCRIPT

393 **References**

394 Ager, D.V., 1993. *The Nature of the Stratigraphical Record*. Wiley, Chichester, UK.

395

396 Baker, V.R., 2003. Icy martian mysteries. *Nature* 426, 779–780.

397

398 Balme, M.R., Gallagher, C.J., Page, D.P., Murray, J.B., Muller, J-P., 2009. Sorted stone circles in Ely-
399 sium Planitia, Mars. *Icarus* 200, 30–38.

400

401 Boisson, J., Heggy, E., Clifford, S.M., Frigeri, A., Plaut, J.J., Picardi, G., 2008. Exploring Athabasca
402 subsurface geoelectrical properties using MARSIS radar data: hypothesis on volcanic or fluvial origin of
403 the local morphology. *Lunar Planet. Sci.* XXXIX. Abstract 1819.

404

405 Boynton, W.V., and 24 colleagues, 2002. Distribution of hydrogen in the near surface of Mars: Evidence
406 for subsurface ice deposits. *Science* 297, 81–85.

407

408 Broeker, W.S., Denton, G.H., 1989. The role of ocean-atmosphere reorganizations in glacial cycles.
409 *Geochim. Cosmochim. Acta* 53, 2465–2501.

410

411 Burr, D.M., Grier, J.A., McEwen, A.S., Keszthelyi, L.P., 2002. Repeated aqueous flooding from the Cer-
412 berus Fossae: Evidence for very recently extant, deep groundwater on Mars. *Icarus* 159, 53–73.

413

414 Burr, D.M., Parker, A.H., 2006. Grjota´ Valles and implications for flood sediment deposition on Mars.

415 *Geophys. Res. Lett.* 33, L22201, doi:10.1029/2006GL028011.

416

417 Cabrol, N.A., Grin, E.A., 2002. The recent Mars Global Warming (MGW) and/or South Pole Advance
418 (SPA) hypothesis: global geological evidence and reasons why gullies could still be forming today. Lu-
419 nar Planet. Sci. XXXIII. Abstract 1058.

420

421 Campbell, B.A., and 13 colleagues, 2007. SHARAD mapping of subsurface geologic horizons in Ama-
422 zonis Planitia. Lunar Planet. Sci. XXXVIII. Abstract 3225.

423

424 Chamberlain, M.A., Boynton, W.V., 2007. Response of Martian ground ice to orbit-induced climate
425 change. J. Geophys. Res. 112, E06009, doi:10.1029/2006JE002801.

426

427 Clifford, S.M., 1998. Mars: The effect of stratigraphic variations in regolith diffusive properties on the
428 evolution and vertical distribution of equatorial ground ice. Lunar Planet. Sci. XXIX. Abstract 1922.

429

430 Costard, F.M., Kargel, J.S., 1995. Outwash plains and thermokarst on Mars. *Icarus* 114, 93–112.

431

432 Deynoux, M., 1982. Periglacial polygonal structures and sand wedges in the Late Precambrian glacial
433 formations of the Taoudeni Basin in Adrar of Mauritania (West Africa). *Palaeogeogr., Palaeoclim., Pa-*
434 *laeoecol.* 39, 55–70.

435

436 Diez, B, Feldman, W.C., Mangold, N., Baratoux, D., Maurice, S., Gasnault, O., d'Uston, L., Costard, F.,
437 2009. Contribution of Mars Odyssey GRS at central Elysium Planitia. *Icarus* 200, 19–29.

438

439 Dylik, J., 1964. Eléments essentials de la notion de 'périglaciale'. *Biuletyn Peryglacjalny* 14, 111–132.

440

441 Emiliani, C., 1955. Pleistocene temperatures. *J. Geol.* 63, 538–578.

442

- 443 Eyles, N., 1993. Earth's glacial record and its tectonic setting. *Earth-Sci. Revs.* 35, 1–248.
444
- 445 Farrand, W.H., Gaddis, L.R., 2003. Themis observations of pitted cones in Acidalia Planitia and Cydo-
446 nia Mensae. *Lunar Planet. Sci. XXXIV*. Abstract 3094.
447
- 448 Feldman, W.C., Head, J.W., Maurice, S., Prettyman, T.H., Elphic, R.C., Funsten, H.O., Lawrence, D.J.,
449 Tokar, R.L., Vaniman, D.T., 2004. Recharge mechanism of near-equatorial hydrogen on Mars: Atmos-
450 pheric redistribution or sub-surface aquifer. *Geophys. Res. Lett.* 31, doi:10.1029/2004GL020661.
451 L18701.
452
- 453 Forte, A.M., Mitrovica, J.X., 1997. A resonance in the Earth's obliquity and precession over the past 20
454 Myr driven by mantle convection. *Nature* 390, 674–680
455
- 456 French, H., 1996. *The Periglacial Environment*, second ed. Longman, Essex.
457
- 458 Hamilton, V. E., Christensen, P. R., McSween, H. Y., Jr., Bandfield, J. L. (2003) Searching for the
459 source regions of martian meteorites using MGS TES: Integrating martian meteorites into the global
460 distribution of igneous materials on Mars. *MAPS* 38 (6), 871-885.
461
- 462 Harris, S.A., 2002. Global heat budget, plate tectonics and climatic change. *Geogr. Ann.* 84, 1–9.
463
- 464 Hartmann, W.K., 1999. Martian cratering VI: Crater count isochrons and evidence for recent volcanism
465 from Mars Global Surveyor. *Meteorit. Planet. Sci.* 34, 167–177.
466
- 467 Hartmann, W.K., 2005. Martian cratering. 8. Isochron refinement and the chronology of Mars. *Icarus*
468 174, 294–320.

- 469 Hartmann, W.K., Berman, D.C., 2000. Elysium Planitia lava flows: Crater count chronology and geo-
470 logical implications. *J. Geophys. Res.* 105, 15011–15026.
- 471
- 472 Hartmann, W.K., Neukum, G., 2001. Cratering chronology and the evolution of Mars. In: Kallenbach, R.,
473 Geiss, J., Hartmann, W.K. (Eds.), *Chronology and Evolution of Mars*. In: *Space Sci. Rev.*, vol. 96. Klu-
474 wer Academic, Norwell, MA, pp. 165–194.
- 475
- 476 Hays, J.D., Imbrie, J., Shackleton, N.J., 1976. Variations in the Earth's orbit: Pacemaker of the ice
477 ages. *Science* 194, 1121–1132.
- 478
- 479 Head, J.W., Marchant, D.R., 2003. Cold-based mountain glaciers on Mars: Western Arsia Mons. *Geol-*
480 *ogy* 31, 641–644.
- 481
- 482 Head, J.W., Mustard, J.F., Kreslavsky, M.A., Milliken, R.E., Marchant, D.R., 2003. Recent ice ages on
483 Mars. *Nature* 426, 797–802.
- 484
- 485 Imbrie, J., Imbrie, J.Z., 1980. Modeling the climatic response to orbital variations. *Science* 207, 943–
486 953.
- 487
- 488 Ivanov, B.A., Neukum, G., Bottke, W.F., Jr., Hartmann, W.K., 2002. The Comparison of Size-Frequency
489 Distributions of Impact Craters and Asteroids and the Planetary Cratering Rate. *Asteroids III*, W. F. Bot-
490 tke Jr., A. Cellino, P. Paolicchi, and R. P. Binzel (eds), University of Arizona Press, Tucson, p.89-101.
- 491
- 492 Jaeger, W.L., Keszthelyi, L.P., McEwen, A.S., Dundas, C.M., Russell, P.S., 2007. Athabasca Valles,
493 Mars: A Lava-Draped Channel System. *Science* 317, 1709–1711.
- 494

495 Jaeger, W.L., Keszthelyi, L., McEwen, A.S., 2008a. Emplacement of Athabasca Valles flood lavas. Lu-
496 nar Planet. Sci. XXXIX. Abstract 1836.

497

498 Jaeger, W.L., Keszthelyi, L.P., McEwen, A.S., Titus, D.N., Dundas, C.M., Russell, P.S., 2008b. Re-
499 sponse to Comment on "Athabasca Valles, Mars: A Lava-Draped Channel System". Science 320,
500 1588c.

501

502 Keszthelyi, L., McEwen, A.S., Thordarson, T., 2000. Terrestrial analogs and thermal models for martian
503 flood lavas. J. Geophys. Res. 105, 15027–15049.

504

505 Levrard, B., Forget, F., Montmessin, F., Laskar, J., 2004. Recent ice-rich deposits formed at high lati-
506 tudes on Mars by sublimation of unstable equatorial ice during low obliquity. Nature 431,1072–1075.

507

508 Liblik, L.K., Moore, T.R., Bubier, J.L., Robinson, S.D., 1997. Methane emissions from wetlands in the
509 zone of discontinuous permafrost: Fort Simpson, Northwest Territories, Canada. Global Biogeochem.
510 Cycles 11, 485–494.

511

512 Mackin, J.H., 1963. The Fabric of Geology (Addison-Wesley, Reading, Mass).

513

514 Malin, M.C., Edgett, K.S., Posiolova, L.V., McColley, S.M., Noe Dobrea, E.Z., Present-day impact cra-
515 tering rate and contemporary gully activity on Mars. Science 314, 1573–1577.

516

517 McEwen, A.S., Preblich, B.S., Turtle, E.P., Artemieva, N.A., Golombek, M.P., Hurst, M., Kirk, R.A., Burr,
518 D.M., Christensen, P.R., 2005. The rayed crater Zunil and interpretations of small impact craters on
519 Mars. Icarus 176, 351–381.

520

- 521 McSween, H.Y., Jr., 2002. The rocks of Mars, from far and near. *MAPS* 37, 7–25.
- 522
- 523 Mellon, M.T., Jakosky, B.M., 1995. The distribution and behaviour of martian ground ice during past
524 and present epochs. *J. Geophys. Res.* 100 (E6), 11781–11799.
- 525
- 526 Mellon, M.T., Feldman, W.C., Prettyman, T.H., 2004. The presence and stability of ground ice in the
527 southern hemisphere of Mars. *Icarus* 169, 324–340.
- 528
- 529 Melosh, H.J., 1989. *Impact Cratering: A Geologic Process* (Oxford Univ. Press, New York).
- 530
- 531 Miall, A.D, Miall, C.E., 2004. Empiricism and model-building in stratigraphy: around the hermeneutic
532 circle in pursuit of stratigraphic correlation. *Stratigraphy* 1, 27–46.
- 533
- 534 Milazzo, M.P., Keszthelyi, L.P., Jaeger, W.L., Rosiek, M., Mattson, S., Verba, C., Beyer, R.A., Geissler,
535 P.E., McEwen, A.S., 2009. Discovery of columnar jointing on Mars. *Geology* 37, 171–174. doi:10.1130/
536 G25187A.1.
- 537
- 538 Mischna, M., Richardson, M.I., Wilson, R.J., McCleese, D.J., 2003. On the orbital forcing of martian wa-
539 ter and CO₂ cycles: A general circulation model study with simplified volatile schemes. *J. Geophys.*
540 *Res.* 108 (E6), doi:10.1029/2003JE002051. 5062.
- 541
- 542 Muller, R.A., MacDonald, G.J., 1997. Spectrum of 100-kyr glacial cycle: Orbital inclination, not eccen-
543 tricity. *Proc. Natl. Acad. Sci.* 94, 8329–9334.
- 544

- 545 Murray, J.B., Muller, J.-P., Neukum, G., Hauber, E., Markiewicz, W.J., Head, J.W., Foing, B.H., Page,
546 D.P., Mitchell, K.L., Portyankina, G., 2005. Evidence from the Mars Express High Resolution Stereo
547 Camera for a frozen sea close to Mars' equator. *Nature* 434, 352–355.
- 548
- 549 Mustard, J.F., Cooper, C.D., Rifkin, M.K., 2001. Evidence for recent climate change on Mars from the
550 identification of youthful near-surface ground ice. *Nature* 412, 411–414.
- 551
- 552 Nyquist, L.E., Bogard, D.D., Shih, C.-Y., Greshake, A., Stöffler, D., Eugster, O., 2001. Ages and geo-
553 logic histories of martian meteorites. In: Kallenbach, R., Geiss, J., Hartmann, W.K. (Eds.), *Chronology*
554 *and Evolution of Mars*. *Space Sci. Rev.* 96. Kluwer Academic, Norwell, MA, 105–164.
- 555
- 556 Orosei, R., Frederico, C., Flamini, E., Frigeri, A., Holt, J.W., Pettinelli, E., Phillips, R.J., Picardi, G., Sa-
557 faeinili, A., Seu, R., 2008. Radar subsurface sounding over the putative frozen sea in Cerberus Palus,
558 Mars. *Geophys. Res. Abs.* 10, EGU2008-A-08952.
- 559
- 560 Osterkamp, T.E., Burn, C.R., 2002. *Encyclopaedia of Atmospheric Sciences* (Academic Press, New
561 York).
- 562
- 563 Page, D.P., Murray, J.B., 2006. Stratigraphical and morphological evidence for pingo genesis in the
564 Cerberus plains. *Icarus* 183, 46–54.
- 565
- 566 Page, D.P., 2007. Recent low-latitude freeze-thaw on Mars. *Icarus* 189, 83–117 (2007).
- 567
- 568 Page, D.P., 2008. Comment on "Athabasca Valles, Mars: A Lava-Draped Channel System". *Science*
569 320, 1588b.
- 570

- 571 P  w  , T.L., 1983. Alpine permafrost in the contiguous United States: a review. *Arctic and Alpine Res.*
572 15, 145–156.
- 573
- 574 Plescia, J.B., 2003. Cerberus Fossae, Elysium, Mars: A source for lava and water. *Icarus* 164, 79–95.
- 575
- 576 Plescia, J.B., 2005. Small-diameter martian craters: Applicability for chronology—Or not. *Lunar Planet.*
577 *Sci.* XXXVI. Abstract 2171.
- 578
- 579 Raymo, M.E., Huybers, P., 2008. Unlocking the mysteries of the ice ages. *Nature* 451, 284–285.
- 580
- 581 Riall, J.A., 1999. Pacemaking the ice ages by frequency modulation of Earth's orbital eccentricity. *Sci-*
582 *ence* 285, 564–568.
- 583
- 584 Rice, J.W., Parker, T.J., Russel, A.J., Knudsen, O., 2002. Morphology of fresh outflow channel deposits
585 on Mars. *Lunar Planet. Sci.* XXXIII. Abstract 2026.
- 586
- 587 Richardson, M.I., McCleese, D.J., Mischna, M., Vasavada, R., 2003. Obliquity, ice sheets, and layered
588 sediments on Mars: what spacecraft observations and climate models are telling us. *Lunar Planet. Sci.*
589 *XXIV.* Abstract 1281.
- 590
- 591 Ruddiman, W.F., Raymo, M., McIntyre, A., 1986. Matuyama 41,000-year cycles: North Atlantic Ocean
592 and northern hemisphere ice sheets. *EPSL* 80, 117–129.
- 593
- 594 Safaeinili, A., and 15 colleagues, 2007. Radio-transparent deposits in the Elysium region of Mars as
595 observed by MARSIS and SHARAD radar sounders. *Lunar Planet. Sci.* XXXVIII. Abstract 3206.
- 596

- 597 Sagan, C., Young, A.T., 1973. Solar neutrinos, martian rivers, and praesepe. *Nature* 243, 459.
598
- 599 Schumm, S.A., 1991. *To interpret the Earth; Ten ways to be wrong*. Cambridge University Press, Cam-
600 bridge.
601
- 602 Shoemaker, E.M., Hackman, R.J., 1962. *The Moon* (Academic Press, New York).
603
- 604 Siebert, N.M., Kargel, J.S., 2001. Small-scale martian polygonal terrain: Implications for liquid surface
605 water. *Geophys. Res. Lett.* 28, 899–902.
606
- 607 Smoluchowski, R., 1968. Mars: Retention of ice. *Science* 159, 1348–1350.
608
- 609 Tanaka K.L., Skinner J.A., Hare T.M., 2005. Geologic map of the Northern Plains of Mars. USGS mis-
610 cellaneous investigation series MAP I-2888.
611
- 612 Veevers, J.J., 1990. Tectonic-climatic supercycle in the billion-year plate-tectonic eon: Permian
613 Pangean icehouse alternates with Cretaceous dispersed-continents greenhouse. *Sedimentary Geol.*
614 68, 1–16
615
- 616 Washburn, A.L., 1980. Permafrost Features as Evidence of Climatic Change. *Earth-Sci. Revs.* 15, 327–
617 402.
618
- 619 Werner, S.C., van Gasselt, S., Neukum, G. 2003. Continual geological activity in Athabasca Valles,
620 Mars, *J. Geophys. Res.*, 108 (E12), 8081, doi:10.1029/2002JE002020.
621

622 Wilhelms, D.E., 1987. The Geologic History of the Moon. *USGS Prof. Pap.* 1348 (U.S. Geological Sur-
623 vey).

624

625 Zhang, T., Barry, R.G., Knowles, K., Heginbottom, J.A., Brown, J., 2008. Statistics and characteristics
626 of permafrost in the northern hemisphere. *Polar Geography* 31, 47-68, 10.1080/10889370802175895.

627

628 Zimbelman, J.R., 2001. Image resolution and evaluation of genetic hypotheses for planetary land-
629 scapes. *Geomorphology* 37, 179–199.

630

631 Zuber, M.T., 2001. The crust and mantle of Mars. *Nature* 412, 220–227.

632

633

634

635

636

637

638

639

640

641

642

643

644

645

646

647

648 **Table and Figure captions**

649 Table 1. Crater count data for Amazonis Planitia (binned by diameter [e.g., 149 craters between 3.91
650 and 5.52 m]) and context map centred on 18°N / 197°E showing count areas. Tabulated data indicate
651 crater numbers in polygonal ground in HiRISE PSP_008092_1980, PSP_008382_1980 and MOC S09-
652 02331, covering 12 km², 2.1 km², and 45.4 km², respectively. A count on less-polygonised terrain
653 (count 4 in context map, black plot in Fig. 2b) was also undertaken to determine if the effects of poly-
654 gonisation could be detected in the SFD. Counts in the context map are shown as lines across the cra-
655 ter diameter (for many of these to be visible, the image will need to be zoomed to maximum). HiRISE
656 counts were individually numbered to allow later separation of the crater population into those that pre-
657 date, postdate, or are indeterminate to, the polygonal sculpture, these subdivisions of the counts plotted
658 as the red (predate) and blue (postdate and indeterminate) SFDs in Fig. 2b (i.e., Groups 1, 2 and 3, re-
659 spectively – see main text). This numbering also allowed counts and stratigraphical designations to be
660 cross-checked among the authors. Counts in MOC (of those areas not covered by HiRISE imagery) do
661 not bear identification numbers as all the craters counted in Fig. 2a and surrounding terrain could be
662 seen to predate formation of the polygonal sculpture at MOC resolution (i.e., are Group 1 craters). Only
663 at HiRISE resolution are the small 'indeterminate' craters visible, along with the majority of those that
664 postdate polygonisation.

665
666 Table 2. Crater count data for Athabasca Valles (binned by diameter [e.g., 105 craters between 3.91
667 and 5.52 m in Platy Area]) and context map centred on 8°N / 153°E showing count areas. Tabulated
668 data indicate crater numbers in platy ground and two areas of polygonal ground in HiRISE PSP_0035
669 71_1880, covering 0.27 km², 2.2 km², and 0.33 km², respectively, along with crater densities for these
670 areas. Last row shows crater density difference (weighted mean) between platy and polygonal grounds.
671 Data plotted as black and blue SFDs in Fig. 2d (main text). Density differences are only presented for
672 diameter bins in the 7.81 m to 22.1 m range, where data were not limited by resolution / small-number
673 statistics. Because of the clear partitioning of craters between platy and polygonal surfaces, this crater

674 population cannot be secondary in origin, derived from a primary impact elsewhere on the surface, as
675 previously suggested for the majority of small impact craters in Athabasca Valles [McEwen et al., 2005].
676 Thus our derived age-difference is robust (also see Appendix A2). Counts in context map shown as
677 lines across the crater diameter (for these to be visible, image will need to be zoomed to maximum).

678

679 Table 3. Geological history of events in platy, polygonally-patterned ground of Athabasca Valles (Figs.
680 2c and 2e), as determined stratigraphically. Ages derived from impact crater SFD as described in text.

681

682 Fig. 1. Context map showing extent of platy, polygonally-patterned ground across Elysium-Amazonis
683 plains (North polar stereographic projection of gridded MOLA data). Locations of Figs. 2 and 4-5 shown
684 in white. Mapped extent of deposits (shown in black) is based on the mapping of Tanaka et al. (2005),
685 extended to all platy, polygonally-patterned terrain found in this study. Although these extended depos-
686 its are notionally of different 'absolute' ages, post-depositional superposition of impact craters has impli-
687 cations for the drawing of all Formational boundaries on Mars on the basis of impact crater density.

688

689 Fig. 2. Age-relations in polygonally-patterned grounds across the Elysium-Amazonis plains. North to
690 top, scale bars = 100 m. All crater counts performed in HiRISE at 25 cm / pixel unless otherwise stated.
691 Chronology and Production Functions for 2b and 2d those of Hartmann and Neukum (2001) and Ivanov
692 et al. (2002), respectively. 2a) polygonal sculpture in Amazonis Planitia superposes 100% of impact
693 craters = postdates craters (composite sub-scene of MOC S09-02331, 3.19 m / pixel, 18°N / 197°E).
694 Inset: detail of polygonal sculpture crossing crater (from HiRISE PSP_008092_1980). 2b) crater count
695 of surface in 2a and surrounding area, divided stratigraphically into craters that postdate (blue, left) and
696 predate (red, middle) polygonal sculpture. Background count in less polygonised terrain (black, right).
697 Isochrons (grey) from left to right: 100 ka, 1 Ma, 10 Ma, 100 Ma, 1 Ga. Note 40-fold age difference be-
698 tween substrate and polygonisation [HiRISE PSP_008092_1980, 25 cm / pixel, 18°N / 197°E]. 2c) im-
699 pact craters concentrated in platy regions of platy, polygonally-patterned ground in Athabasca Valles =

700 platy and polygonal surfaces formed at different times [HiRISE PSP_003083_1890, 25 cm / pixel, 9°N /
 701 155°E]. 2d) crater count of polygonal (blue, left) and platy (black, right) surfaces in 2e. Note age differ-
 702 ence, cf. 2b. 2e) geological history of platy, polygonal ground in Athabasca Valles. Craters again con-
 703 centrated in platy regions and sparse in polygonal areas: crater density 10-20x greater in platy than po-
 704 lygonal ground = polygonal ground younger; pitted cones cross-cut both = postdate both. Note indica-
 705 tion of long-term mound growth: 'wakes' formed downstream from earlier mounds severed where plates
 706 rafted apart (white arrows), and two post-fracture mounds developing across the breach between platy
 707 and polygonal ground (dark arrows) [HiRISE PSP_003571_1880, 7.5°N / 153°E].

708

709 Fig. 3. Schematic vertical cross-sections of generalised 'layer-cake' stratigraphy with impact crater (3a)
 710 and stratigraphy of cratered polygonal ground in the Amazonis plain (3b). The crater in 3b is a 'Group 1'
 711 crater (see main text section 'Geochronology' for explanation).

712

713 Fig. 4. Periglacial landform assemblage showing secondary age-relations relative to impact craters.
 714 North to top, scale bars = 100 m, all images from HiRISE at 25 cm / pixel. 4a) polygonal surface sculp-
 715 ture in Amazonis plain cross-cutting crater on SW side (= postdates crater). Note presence of sculpture
 716 on crater floor (light arrow), continuous with that outside the crater (lower arrow): an unambiguous indi-
 717 cator of relative age [PSP_008382_1980, 18°N / 197°E]. 4b) polygonal surface sculpture in Amazonis
 718 plain subdued in vicinity of crater rim and proximal ejecta, suggesting that crater postdates polygonisa-
 719 tion [PSP_008092_1980, 18°N / 197°E]. 4c) pitted mounds in Athabasca Valles, comparable to terres-
 720 trial pingos, intrude wall of impact crater (light arrow) = postdates crater [PSP_002147_1875, 7.5°N /
 721 153°E]. 4d) pitted mound within thermokarst-like collapse structure in Athabasca Valles; wall of collapse
 722 structure transects crater rim (light arrow) = postdates crater [PSP_001540_1890, 9°N / 156°E]. 4e) sur-
 723 face ridging, comparable to solifluction lobes on Earth, sweeps over impact crater in Athabasca Valles
 724 (ridge front arrowed) = postdates crater [PSP_003571_1880, 7.5°N / 153°E]. 4f) sorted stones circles in
 725 Athabasca Valles, a clastic sedimentary structure diagnostic of freeze-thaw cycling on Earth [PSP_

726 004072_1845, 4.5°N / 156°E]. 4g) polygonal sculpture in Amazonis plain forms within and along den-
727 dritic drainage channels (light arrows) = postdates channel [PSP_002000_2025, 22°N / 203°E].

728

729 Fig. 5. Polygonal ground-thermokarst-pingo landform association on Earth and analogous assemblage
730 across Elysium-Amazonis plains. North to top, scale bars = 100 m, all Mars images from HiRISE at 25
731 cm / pixel. 5a-b) Degraded pingo in thermokarst lake, Tuktoyaktuk peninsula, Canadian arctic. Note
732 rapid rate of evolution (peripheral thaw slump, loss of ice core). 5c-d) Degraded pingo-like mounds on
733 Mars, each with marginal slump, cf. 5a-b. 5e) LIDAR image of young arctic pingo. 5f-h) Un-degraded
734 pingo-like mounds on Mars, small size / lack of degradation both features consistent with early pingo
735 genesis (cf. 5e and 2e). 5a: NAPL. 5b: from Osterkamp and Burn (2002). 5c: PSP_008382_1980, 18°N
736 / 197°E. 5d: PSP_009675_2060, 25°N / 171°E. 5e: Airborne Imaging Inc. 5f: PSP_007802_2030, 23°N
737 / 195°E. 5g: PSP_002661_1895, 10°N / 156°E. 5h: PSP_003083_1890, 9°N / 155°E.

738

739 Fig. 6. Variation in martian obliquity during period of polygonal ground formation. 6a) Obliquity variation
740 over the past 20 Ma with model boundaries of equatorial ground ice stability (dark grey, > 30°) and in-
741 stability (light grey, < 30°) marked. 6b) Detail of 6a showing decrease in obliquity at 5 Ma, correspond-
742 ing to dated period of surface polygonisation across Elysium-Amazonis [data from Levrard et al., 2004].

743

744

745

746

747

748

749

750

751

752

Method and Appendix

753

A1. Geological determination of relative age

755 While our derived surface ages or geochronology of events in the Elysium-Amazonis plains are
756 based on impact crater counts, they were made with an eye to relative age first – that is, chronostrati-
757 graphically. An analogy illustrative of the distinction between relative and absolute age can be found in
758 Earth's Colorado Plateau and Grand Canyon. While improvements in dating techniques may give us an
759 ever-finer estimate of the absolute age of canyon formation (geochronology), the age of the canyon
760 relative to the plateau through which it cuts remains the same – it formed later (chronostratigraphy).
761 This relative age-dating is fundamental, serving as a check of derived ages and a more structural way
762 of looking at the age of planetary surfaces. Clearly, a total crater count of the surfaces in Figs. 2a, 2c or
763 2e (main text) would give a very misleading impression of true surface age and geological history.

764

765 Our determinations of relative age were made on the basis of stratigraphy (principally) and im-
766 pact energetics. If a surface landform (i.e., polygonal sculpture, pitted cone, collapse feature or surface
767 ridge (see Fig. 4, main text) was observed to reach a crater rim, it was judged to postdate that crater.
768 The justification for this is two-fold: stratigraphically, the material forming the rim of an impact crater was
769 not in its current position prior to impact – it is allochthonous material excavated from the crater bowl
770 and emplaced during the impact event. While it is conceivable that pre-existing surface features might
771 survive such impact, the material forming the rim forced out en-masse (i.e., structural rather than ballis-
772 tic emplacement: a suitable analogy being a house that remains intact on a land-slipped surface), the
773 presence of the polygonal sculpture *within* the crater basin, continuous with that outside the crater, ef-
774 fectively precludes this possibility. This is the fundamental stratigraphical approach of terrestrial geology
775 [Mackin, 1963], as applied on the Moon [Shoemaker and Hackman, 1962], where any structure that
776 cross-cuts an impact crater rim is a sign of relative age in all but the most contrived scenarios [Wil-
777 helms, 1987]. Examples of such intra-crater polygonisation are shown in Figs. A1a-b; e-h herein.

778 Preservation of pre-existing surface structure within a crater rim is nowhere observed in nature,
779 nor experimentally; neither is it an expectation of theory [Melosh, 1989]. This is the case whether the
780 impacting object is a primary projectile travelling at cosmic velocity ($> 11 \text{ km s}^{-1}$), or secondary material
781 from a primary impact elsewhere on the surface, arriving at much slower speeds (e.g., $\sim 500 \text{ m s}^{-1}$). Al-
782 though the possibility of slow, secondary impacts conservative of surface features is often given in de-
783 fence of the antiquity of the Elysium landforms [e.g., Jaeger et al., 2007, 2008b], it remains the case
784 that a slower projectile, i.e., one with less kinetic energy, must be larger to excavate a crater of equiva-
785 lent size. Where a 50 cm projectile may form a 50 m crater at hypervelocity, a m- to dm-scale projectile
786 is required to achieve the same effect at slower speeds. As impact velocity decreases to 100s of m s^{-1} ,
787 the crater formed is eventually no bigger than the impactor itself, and a direct hit on all landforms within
788 the crater radius results. Hence, whether the crater seen at the surface is the result of a hypervelocity
789 impact wave propagating out from ground zero, or is the product of a slower but much larger object
790 physically impacting everything within the impact radius, nothing is preserved within the rim. Thus the
791 presence of each of these martian landforms within the crater bowl is the justification for our methodol-
792 ogy of stratigraphically-controlled impact crater counts, whereby if a landform cuts the crater rim, it is
793 post-depositional.

794

795 Page (2008) showed an example of a such a 'direct hit' upon one of the pingo-like features in
796 Athabasca Valles, reproduced here as Fig. A1d. The result of such an impact is that all surface struc-
797 ture is obliterated out to ~ 1.5 crater radii [see Melosh, 1989; Page and Murray, 2006]. Given all possi-
798 ble combinations of lithology and impact velocity, preservation of pre-existing surface features would
799 seem to be possible, but the simpler explanation – that these structures are post-depositional – is
800 clearly more likely given that we would have to invoke an alternative explanation for every single exam-
801 ple of this superposition (and there are more than a hundred visible in Fig. 2a [main text] alone and
802 thousands of such examples in these deposits regionally), expressed by an entire assemblage of con-
803 structural and degradational landforms (Fig. 4, main text). It is only the general preconception we have

804 of these deposits – that these are lava flows – that stands in the way of the conclusion that the features
805 within them are post-depositional, as highlighted by the large variations in impact crater density on sur-
806 faces previously assumed to be co-genetic [e.g., Plescia, 2003; Werner et al., 2003].

807

808 These structural observations are entirely consistent with the differences between the two com-
809 peting hypotheses of origin. Lava flows and their associated landforms have their geomorphological
810 characteristics established in the time it takes them to crystallise; thereafter, they are only subject to
811 modification by erosion or burial. In contrast, periglacial landforms and landscapes are the product of
812 continuous, often repetitious, constructional and degradational processes; as such, they can interact
813 stratigraphically with post-depositional structures, such as impact craters, in a way that solid rock can-
814 not. The age-gap (or disconformity) between substrate and polygon formation in the Amazonis plain is
815 also evident in Athabasca Valles, 2000 km to the west, where the age relations are much less subtle.

816

817 Part of the change in perspective that looking at the impact crater population stratigraphically
818 brings is to recognise that the craters we see at the surface are what is left after geological processing;
819 that geology will often determine what we infer from such populations. Some workers have suggested
820 that flattening of the small-crater SFD, recognised for some time in the Elysium plain [e.g., Hartmann
821 and Neukum, 2001; Hartmann and Berman, 2000; Burr et al., 2002; Plescia, 2005] and now extended
822 to the Amazonis plain, is the product of an imperfectly understood production function and that age-
823 dating based on small craters is unreliable as a result [Plescia, 2005], particularly in regard to recent
824 climate change [McEwen et al., 2005]. This is not borne out by observations of craters that have formed
825 on Mars within the last decade [Malin et al., 2006], or that the loss of small craters seen in the Elysium-
826 Amazonis plain is not replicated on the volcanic constructs of the Elysium-Tharsis Montes [Hartmann,
827 1999]. It is however what would be expected in terrain where endogenous geological activity is destruc-
828 tive of impact craters [Page, 2007], and consistent with the diameter-dependent obliteration we have
829 observed in these deposits.

830 For instance, the largest crater in Fig. 2a (at far left) is clearly superposed by the polygonal
831 sculpture, but still recognisably an impact crater. Go to the smaller inset crater of this figure (duplicated
832 here as Fig. A1b) and notice how softened the crater outline is by polygon formation – cover the un-
833 polygonised (upper-right) part of the crater with the hand and we would not even know it is there; the
834 rim at lower-left is all but gone. Given the destructive nature of intrusive polygonisation, it is entirely
835 likely that this process is responsible for the flattening of the SFD at small-crater diameter, either by
836 physical loss of craters or obscuration of their detection [cf. Hartmann, 2005; Plescia, 2005]. Not every
837 crater can be constrained in this way, and it is clear that many of the stratigraphically-indeterminate cra-
838 ters (e.g., Fig. A1c, herein) may actually predate polygon formation – geologically (and chronologically),
839 there is no way to tell. However, by placing these craters with the 'postdate' fraction of impact craters
840 (Group 2 [see main text]) we over-estimate the age of all the youngest craters, avoiding any bias toward
841 a younger age in our results: a useful safeguard in an investigation of recent surface activity.

842

843 Note that because the polygonal sculpture postdates the vast majority of impact craters in these
844 deposits, the primary or secondary origin of the impacting projectiles is effectively irrelevant in terms of
845 relative age, the degree of 'contamination' resulting from such secondaries where much of the debate in
846 impact crater chronology currently resides [see Hartmann, 1999; McEwen et al., 2005; Hartmann, 2005;
847 Plescia, 2005; Malin et al., 2006]. The same argument is also applicable to 'absolute' age (see A2).

848

849 **A2. Geology and determination of absolute age**

850 We must consider the possibility that our measured chronology is wrong. However, the majority
851 of impact craters in the study area are either transected by periglacial landforms (Fig. 2a main text, Fig.
852 A1 herein) or concentrated in the platy, non-periglacial lithologies (Fig. 2c,e main text), so if the crater
853 numbers speak of the passage of 100s of millions of years, then these polygonal surfaces are the
854 product of change in no more than the last few percent of that time. This observation is independent of
855 the cratering chronology model used, or any systematic error in those chronologies at the diameters

856 observed [Hartmann and Neukum, 2001; Hartmann, 2005]. As nearly 100% of the Amazonis craters are
857 deformed by polygonisation (Fig. 2a, main text), this deformation must be young. This conclusion holds
858 even if 100% of these craters are secondaries, in which case polygon formation can still be said to be
859 younger than the secondary-causing impact event. Furthermore, the uneven distribution of small impact
860 craters between adjoining platy and polygonal lithologies in Athabasca Valles indicates that this crater
861 population cannot be the product of temporally-restricted secondary impact, as might result from a large
862 primary impactor showering the region in secondary projectiles on a scale of hours (as suggested for
863 the majority [~ 80%] of small impact craters within the Athabasca Valles channel [McEwen et al.,
864 2005]). These temporal non-conformities, geographically (i.e., laterally) in Athabasca Valles, and strati-
865 graphically (i.e., vertically) in Amazonis, are the clearest indication that the surface deposits of the Cer-
866 berus Formation are not solid rock.

867

868 Clearly, there is a danger in using crater chronology to date deposits in which it can be shown
869 that many of the geological assumptions made by that chronology (i.e., a rocky surface of uniform age
870 preserving a 'production population' of impact craters [Hartmann and Neukum, 2001]) do not apply, the
871 decoupling of surface age from bulk crater statistics in Fig. 2 one manifestation of this. However, the
872 theoretical justification for making counts at the surface – i.e., the asteroidal production function – still
873 exists, so impact craters may still be relied on to date that process if the counts are stratigraphically-
874 controlled, the martian isochrons having their origin in the lunar production function where such compli-
875 cations as periglacial overprinting do not arise. The implications of this time-transgressive activity in the
876 type area for martian impact crater chronology are considered in the final section of the Appendix (A5).

877

878 **A3. Distinguishing impact craters from depressions of non-impact origin**

879 Surface depressions of presumed thermokarstic origin are common in these deposits (and one
880 of the signs of periglaciation therein). As Figs. A2a-b show, these depressions are easily distinguished
881 from impact craters because of their irregular or reniform outlines. However, when they are circular in

882 shape (e.g., A2c) they become easy to mistake for impact craters. Fortunately, a number of features
883 exist in both classes of landform that distinguish these depressions from impact craters.

884

885 Fig. A2 shows a circular thermokarst pit (A2c) alongside an impact crater (A2d), the crater a de-
886 graded example with subdued ejecta to facilitate comparison. The impact crater has the characteristic
887 rim raised above the surrounding terrain, forming the classic bowl shape dipping into the centre of the
888 structure. The depression in A2c, however is flat, having no raised rim, and dips steeply down to the
889 floor (such flat-floored pits consistent with an evaporative or sublimative origin [e.g., Page, 2007]). Note
890 also how polygon formation in A2c is orthogonal to the pit margin, at approximate right angles to the
891 periphery, another characteristic of the thermal influence of thermokarst which impact structures do not
892 display. Furthermore, these pits are coalescent where they meet, as A2b demonstrates, unlike impact
893 processes, which overprint each other at their margins (or result in characteristic interference patterns
894 at lower velocities [Melosh, 1989]). Lastly, these depressions are often host to pingo-like pitted cones,
895 as in A2a-b (also Figs. 4-5, main text), an association characteristic of intrusive ground ice processes,
896 not impact (or volcanism).

897

898 **A4. Detection of ground ice**

899 If the deposits of the Elysium-Amazonis plains have an icy origin, where is this ice? The current
900 generation of orbiting spectrometers and radars provide inconclusive results with regard to this ques-
901 tion. The Mars Odyssey Gamma-Ray Spectrometer is unable to sense hydrogen below ~ 1 m depth,
902 falling below detection limits equatorward of +/- 45° latitude [Boynton et al., 2002]. The radars MARSIS
903 and SHARAD, aboard *Mars Express* and *Mars Reconnaissance Orbiter* respectively, are capable of
904 sensing to much greater depth, detecting dielectric discontinuities in the subsurface that could indicate
905 the presence of buried ground ice. While both instruments have provided evidence of a shallow (< 300
906 m) radio-transparent deposit covering the Elysium-Amazonis region, interpretation of this result remains
907 undecided [Safaeinili et al., 2007; Campbell et al., 2007]. However, our observations of this region are

908 of a degraded landscape, perhaps one largely depleted of its volatiles with only patches of recent
909 ground ice activity, and here the SHARAD results are intriguing. Low-loss surface materials in Atha-
910 basca Valles occur in small patches, the largest of which are centred around 5°N / 152°E [Orosei et al.,
911 2008], the region of suggested recent pingo genesis (~7°N / 152°E [Page and Murray, 2006]). The most
912 recent MARSIS soundings of this region [e.g., Boisson et al., 2008] are as consistent with an ice con-
913 tent of ~ 20% (a value well within the range of high-latitude, continuous permafrost on Earth [Zhang et
914 al., 2008]) as they are with 0% ice content, and therefore tell us little about the presence of ground ice
915 in this region.

916

917 **A5. Implications of a revised geology in the Elysium-Amazonis plains**

918 A revised geology at low martian latitude is not just a question of the origin of a single geological
919 formation. The general theory of 'plains-forming' volcanism in this region has become a paradigm of
920 martian geology basal to most ideas of surface processes, impact crater chronology, meteorite source
921 region and thermal evolution. Thus, it is widely considered (effectively by default [McSween, 2002]) that
922 this region must be the source of the young martian (shergottite) meteorites because there are no other
923 regions of widespread, young lava that would satisfy multiple, random ejections of compositionally iden-
924 tical meteorites, concordant in age. Yet, such complex launch scenarios are largely speculative, their
925 basis in derived exposure ages equally consistent with fewer launch events and break-up in transit [Ny-
926 quist et al., 2001], a simpler scenario consistent with the absence of a spectral signal for these meteor-
927 ites anywhere on the martian surface [e.g., Hamilton et al., 2003].

928

929 Similarly, impact crater chronology relies on an assumption of young volcanic plains in this re-
930 gion for testing and refinement of surface isochrons [see Hartmann and Neukum (2001) and Hartmann
931 (2005)], such deposits theoretically preservative of an impact crater population reflective of the impactor
932 population that produced them. Surface units defined on the basis of visual similarity to lava flows, and
933 therefore assumed to be of uniform age, result in composite ages that mask evidence for recent surface

934 activity whilst embedding substantial dating errors within the system (at least at small crater diameter,
935 where the youngest ages are determined). As we have shown, a vast time gap exists within the depos-
936 its of the Elysium-Amazonis plains, one almost as long as their accepted ~ 100 Ma age (literally 'more
937 gap than record' [Ager, 1993]), something that we have found at both geographical limits of their expo-
938 sure. These deposits are not isochronous surfaces, but are markedly diachronous, and unsuitable for
939 isochron construction, especially for the smaller part of the SFD where crater loss is most significant.

940

941 While it can no longer be reasonably maintained that the deposits of this region are lava flows, it
942 would be an overgeneralisation to conclude that this region is non-volcanic. The Elysium-Amazonis pla-
943 ins are host to the solar system's largest volcanoes, magmatic constructs whose effusive products must
944 have gone somewhere. However, this is not cause to relate all that we see at the surface to lava flow
945 [cf., Milazzo et al., 2009; Diez et al., 2009]. This region could be covered with a clastic veneer sufficient
946 to create the platy, polygonal, and conical landforms – our point is simply that it is not composed of lava
947 flows as exposed at the surface. Extrusive rocks do not show these large disconformities and diachron-
948 eities across their surfaces on Earth, and there is no reason to expect this to be the case elsewhere.

949

950 Mars might be formed almost entirely of shergottitic lava, metres-deep in dusty, spectrally-
951 homogenous volcanogenic regolith. Ultimately though, this is reasoning on the basis of negative evi-
952 dence as regards the origin of the Elysium-Amazonis plains, leaving big gaps in the story that ideas of
953 surface chronology and meteorite source region are then made consistent with – a paradigm of geology
954 with no geological foundation, the over-arching nature of which is used to refute all counter-argument.
955 This general theory bears on the larger issue of how we inquire into the nature and age of planetary
956 surfaces and how we reconcile these with the samples in our possession that we believe to be from
957 these planets (not to mention the guide that such studies provide for landed space missions). It is time
958 to critically re-examine the geology of this region and all of the morphological, chronological, and mete-
959 oritical inferences that have been built upon the paradigm of young, 'plains-forming' volcanism on Mars.

960 **Appendix Figure captions**

961 Fig. A1. Polygonal surface sculpture and pitted cones showing age relations relative to impact craters.
962 North to top, scale bars = 100 m. A1a-b) polygonal sculpture in Amazonis Planitia superposing impact
963 craters. Note presence of polygonal sculpture on crater floor in A1b (upper arrow), continuous with that
964 outside crater (lower arrow) = unambiguous indicator of relative age [HiRISE PSP_008092_1980 and
965 PSP_008382_1980, 18°N / 197°E]. A1c) Small, stratigraphically-indeterminate ('Group 3') crater [image
966 details as for A1b]. A1d) pitted cone obliterated by impact. Note loss of pre-existing surface features
967 within crater radius (cf. main text Figs. 4c-d) and presence of un-pitted cone at lower left, cf. main text
968 Figs 5g-h [HiRISE PSP_002661_1895, 9.5°N / 156°E]. A1e-h) Intra-crater polygonal sculpture. The
969 common NW-SE strike of this intra-crater polygonisation may be a product of aeolian etching, normal to
970 the dominant northeasterly wind direction in the Cerberus region [image details as for A1a].

971
972 Fig. A2. Circular-sub-circular structures of impact and non-impact origin in Amazonis Planitia. North to
973 top, scale bars = 100 m. Context views at right, all images from HiRISE at 25 cm / pixel. A2a-b) ther-
974 mokerst-like pitting with centrally located pingo-like mounds, two pits coalescent in A2b. A2c) circular
975 thermokerst-like pit, easily confused with impact crater (cf. A2d). Note characteristics of depression that
976 distinguish this from impact structures: flat floor, no raised-rim or ejecta, and orthogonal polygon forma-
977 tion perpendicular to pit margin (the thermal influence of standing water on subsequent polygonisation
978 resulting in such directed polygon formation in terrestrial thermokerst [French, 1996]). A2d) degraded
979 impact crater for comparison with A2c. Note raised-rim, crescentic, bowl-shaped interior and absence in
980 this impact structure of all aforementioned characteristics of A2a-c [A2a-b: PSP_008382_1980, 18°N /
981 197°E; A2c-d: PSP_008092_1980, 18°N / 197°E].

982

983

984

985

Stratigraphy	Number of craters per bin $\leq D$ (metres)														
	3.91	5.52	7.81	11.05	15.63	22.10	31.25	44.19	62.50	88.39	125.00	176.78	250.00	343.55	500.00
Area 1 All (inc. predate)	17	149	490	596	366	208	77	42	22	11	4	2	-	-	-
Area 1 Indeterminate	7	29	71	30	10	2	-	-	-	-	-	-	-	-	-
Area 1 Postdate	-	1	3	8	2	2	1	1	-	-	-	-	-	-	-
Area 2 All (inc. predate)	5	655	164	135	70	31	14	5	3	-	1	-	-	-	-
Area 2 Indeterminate	4	11	37	19	7	1	-	-	-	-	-	-	-	-	-
Area 2 Postdate	-	4	5	6	3	1	-	-	-	-	-	-	-	-	-
Area 3 All (inc. predate)	-	-	-	-	-	11	64	104	67	21	18	2	2	-	1
Area 3 Indeterminate	-	-	-	-	-	-	-	-	-	-	-	-	-	-	-
Area 3 Postdate	-	-	-	-	-	-	-	-	-	-	1	-	-	-	-
Area 4 All (inc. predate)	-	1	25	87	104	85	41	34	10	3	2	1	-	-	-

Table 1. Data table for impact crater counts in Fig. 2a region of Amazonis Planitia, subdivided stratigraphically (see text).

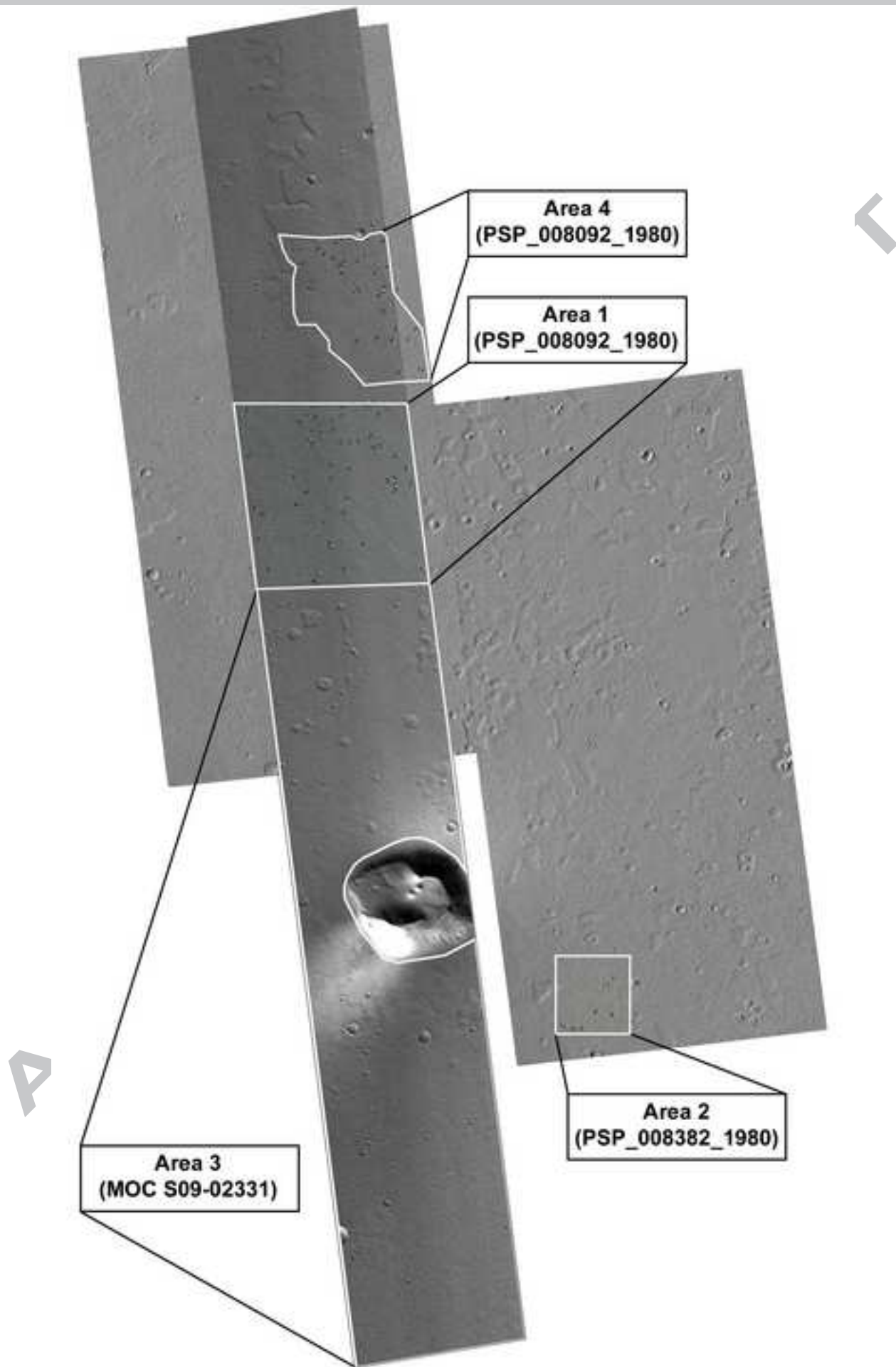
Stratigraphy	Number of craters per bin $\leq D$ (metres)							
	3.91	5.52	7.81	11.05	15.63	22.10	31.25	44.19
Platy Area (density / km ²)	24 (90.6)	105 (396)	155 (585)	75 (283)	25 (94.4)	4 (15.1)	-	1 (3.8)
Polygonal Area 1 (density / km ²)	8 (24.5)	32 (98)	37 (113)	17 (52.1)	21 (6.12)	1 (3.06)	1 (3.06)	-
Polygonal Area 2 (density / km ²)	-	2 (0.92)	33 (15.2)	37 (17)	11 (5.06)	4 (1.84)	2 (0.92)	-
Density difference	-	-	20.9x	13.1x	18.2x	17.6x	-	-

Table 2. Data table for impact crater counts in platy and polygonal ground of Athabasca Valles.

Event	Timing (Ma)
1. platy ground formation and early mound growth, coeval with plate movement (intra-plate wakes)	> ~ 90
2. break-up of plates, severing wakes at plate boundaries	< 90 - > 5
3. polygonal ground formation (essentially uncratered)	~ 5
4. new mound growth, cross-cutting platy and polygonal ground	< 5

ACCEPTED MANUSCRIPT

Table 3. Geological history of events in Athabasca Valles (Fig. 2e).



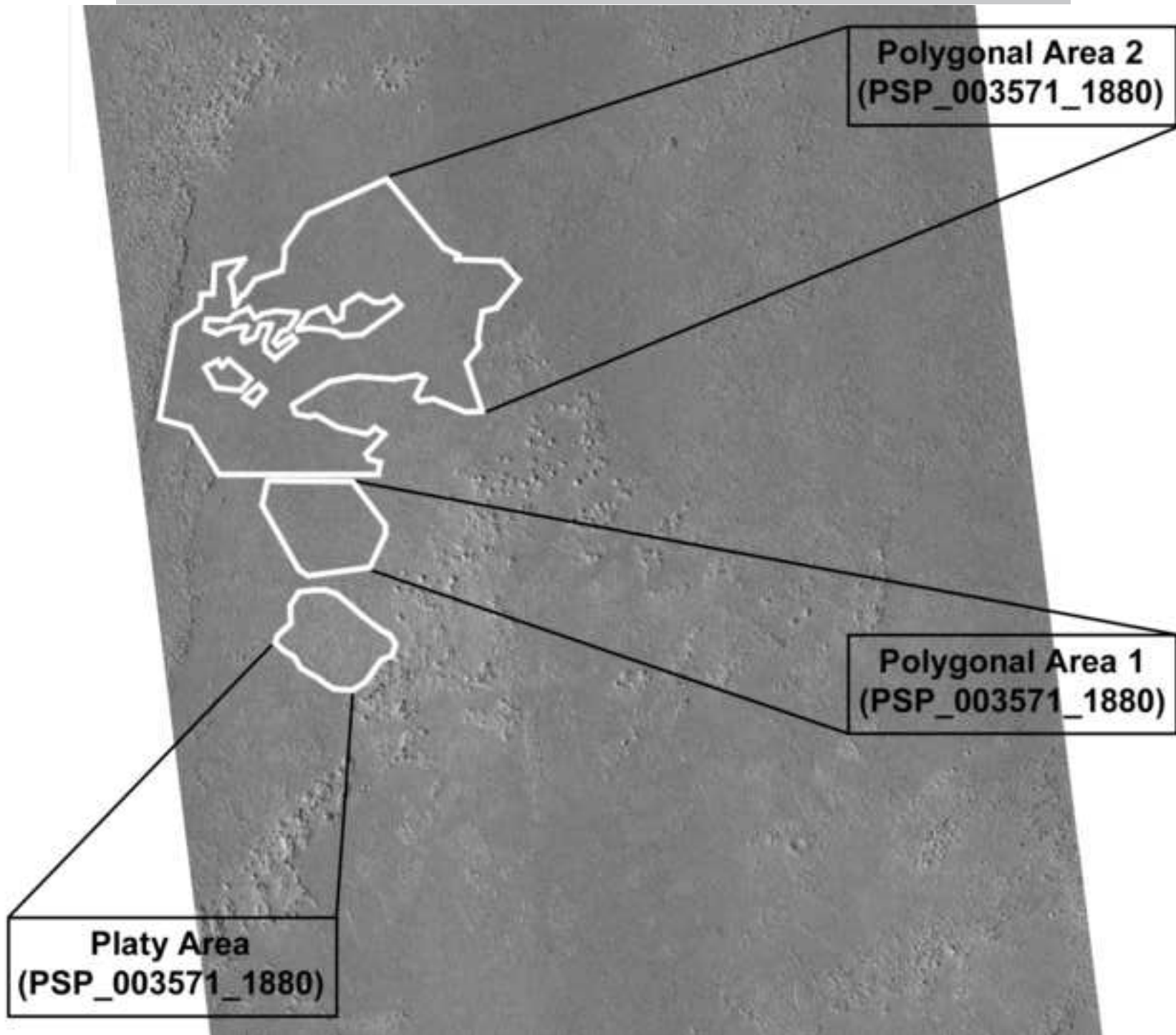
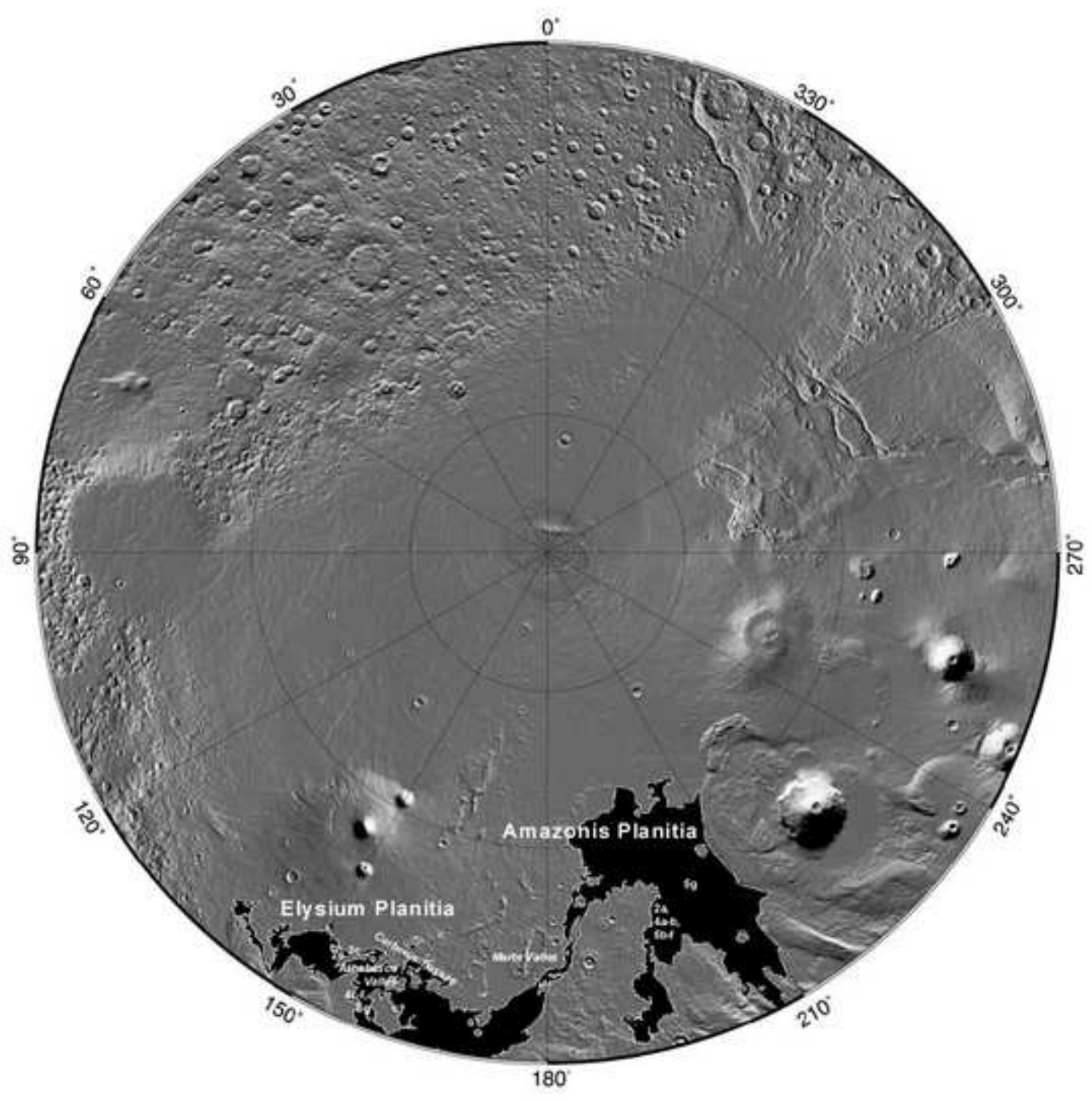
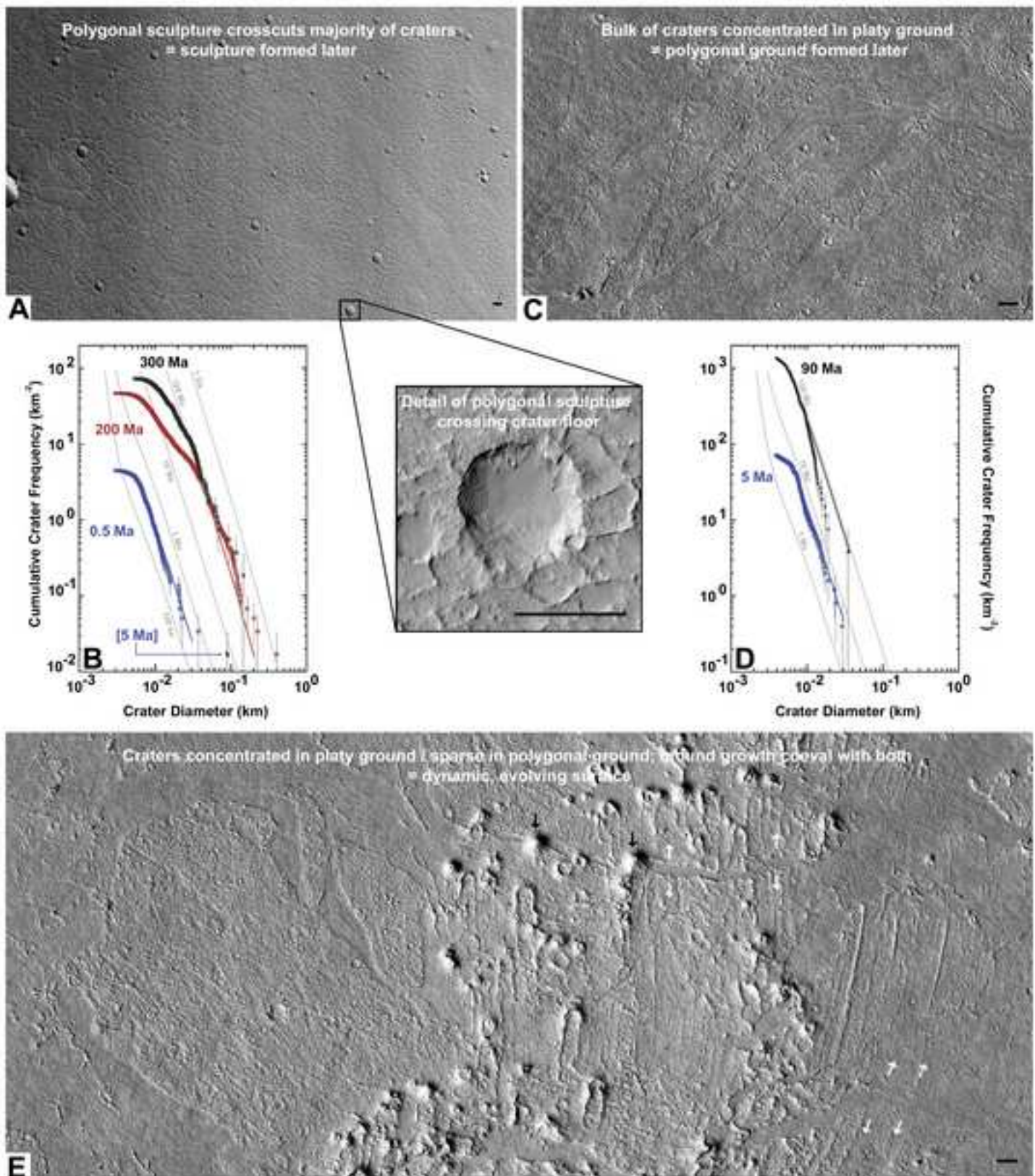
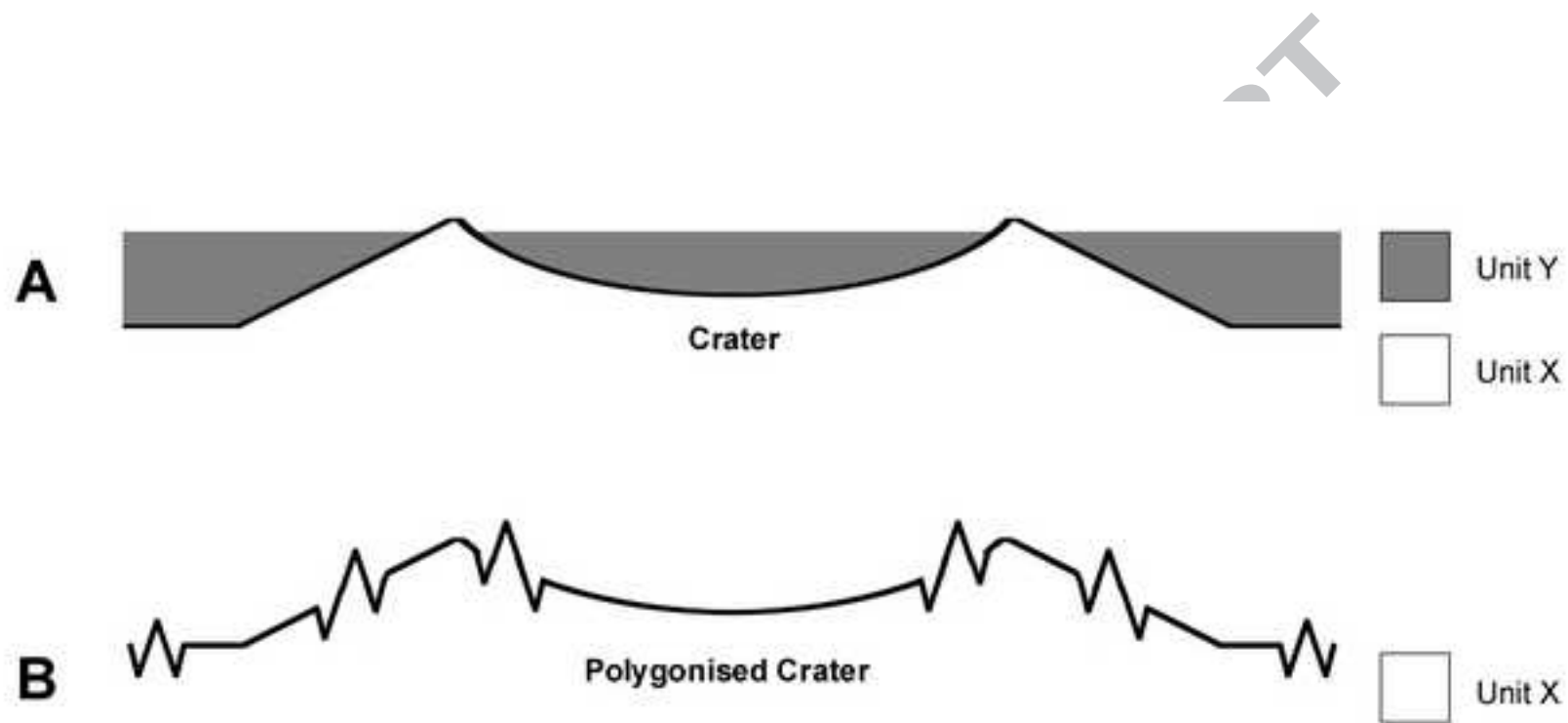
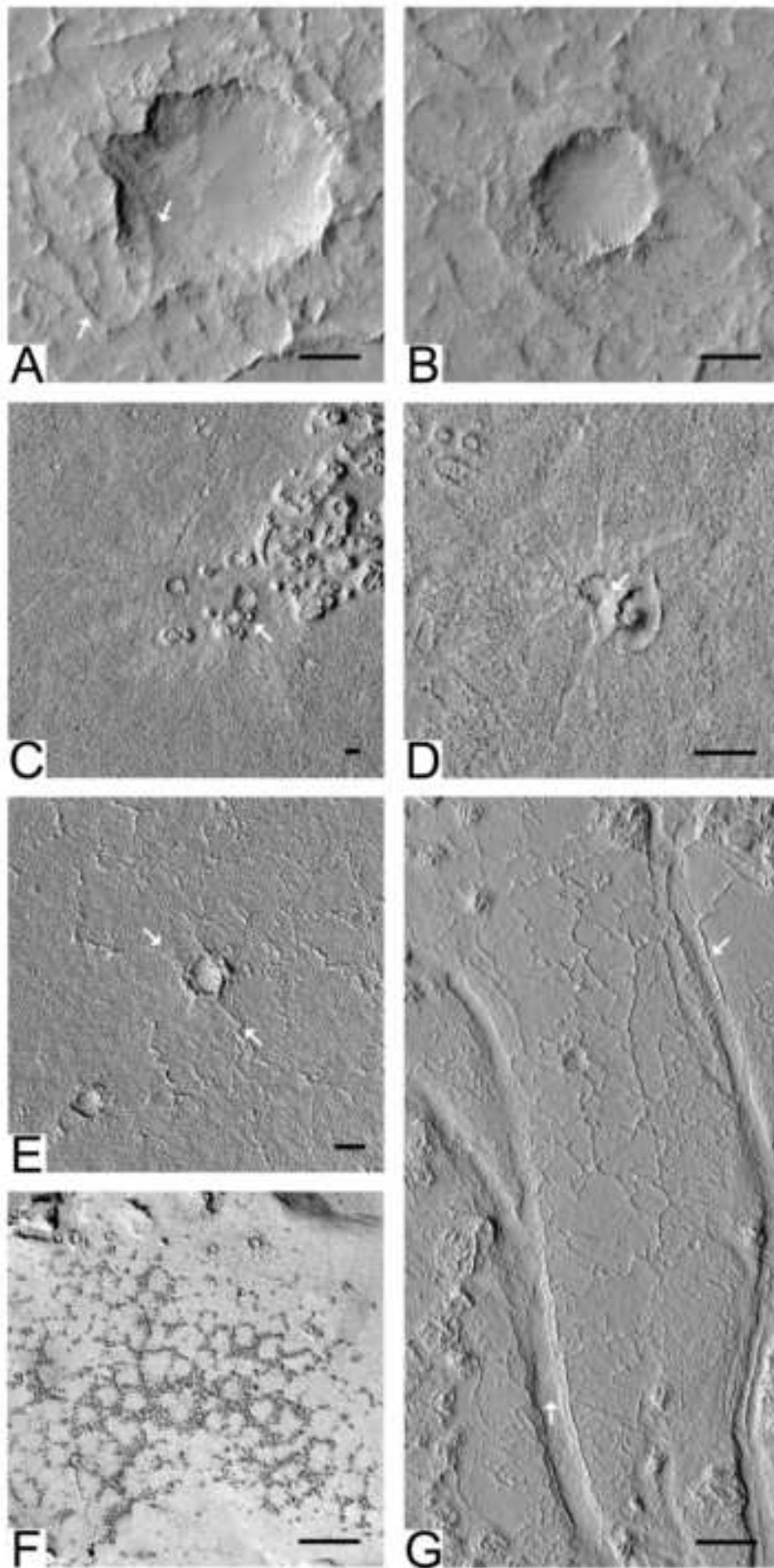


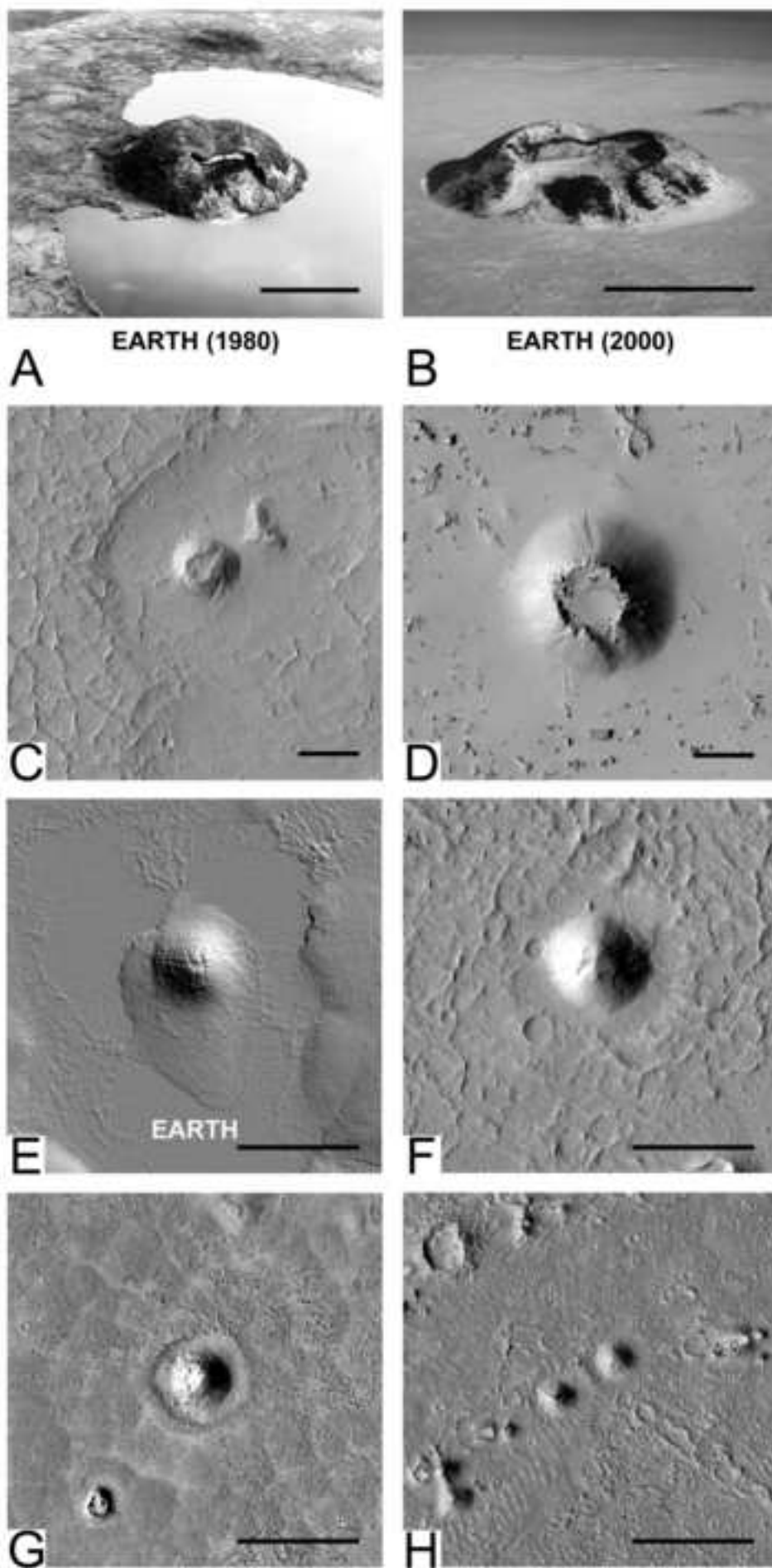
Figure 1

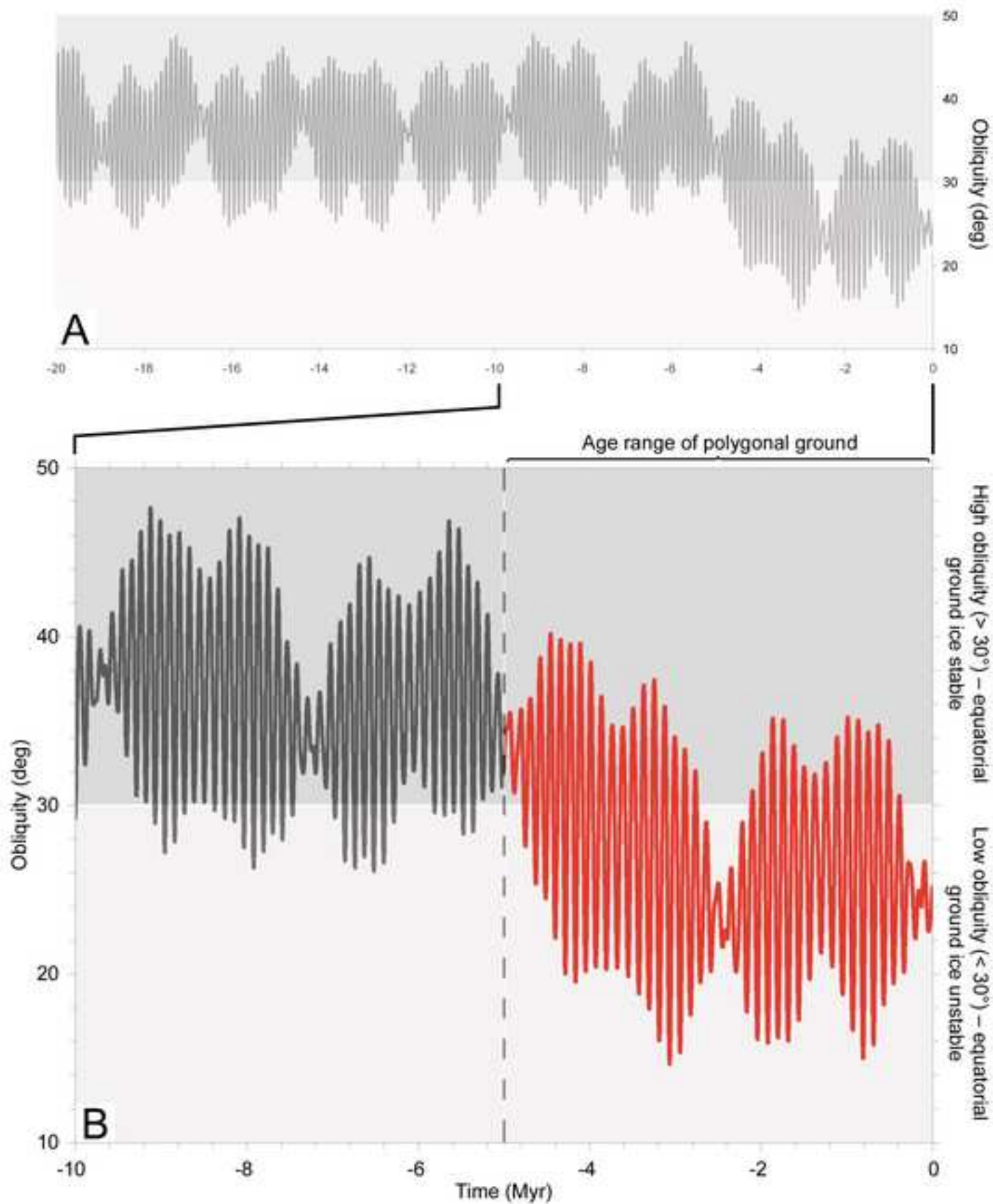


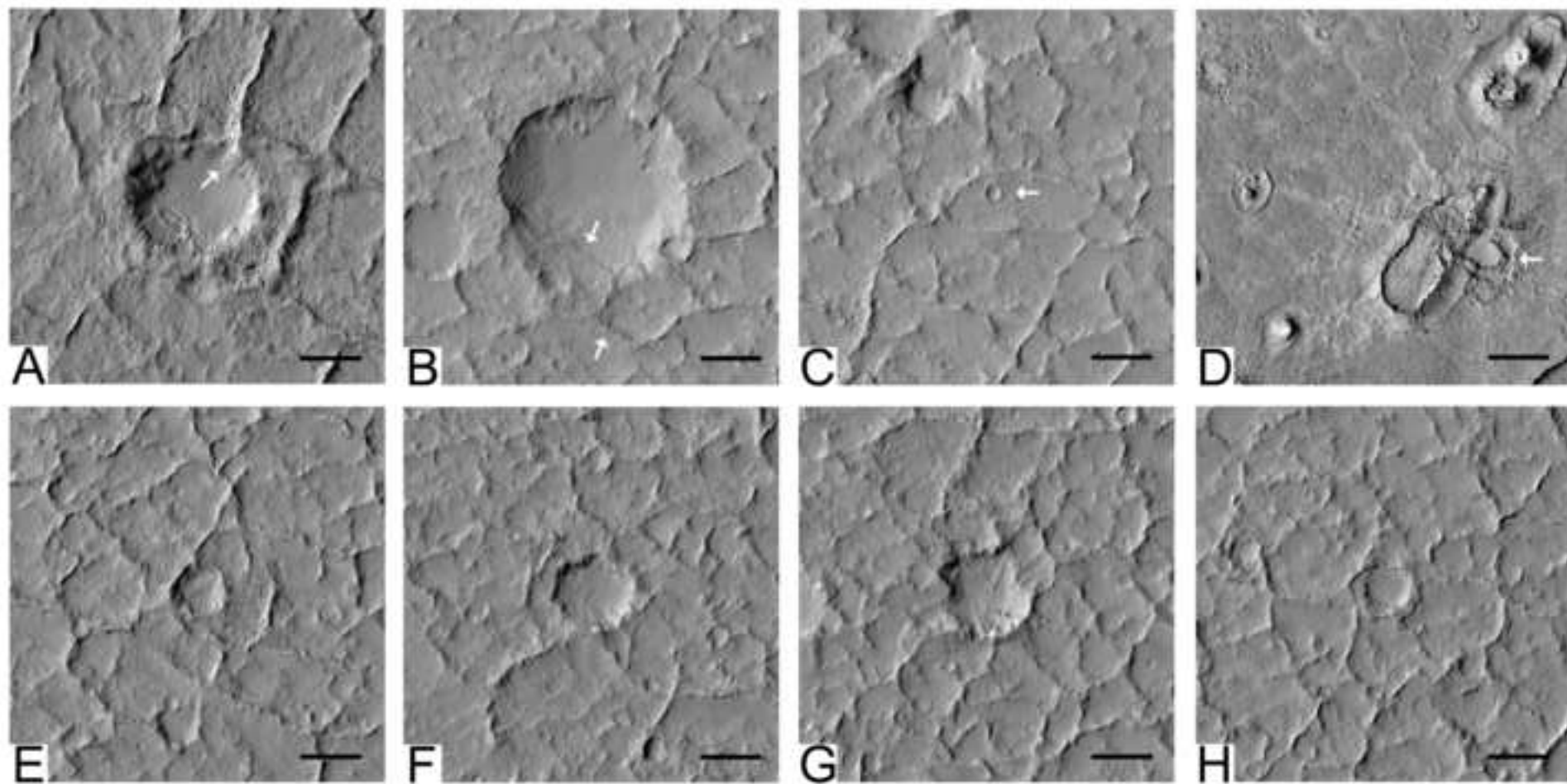


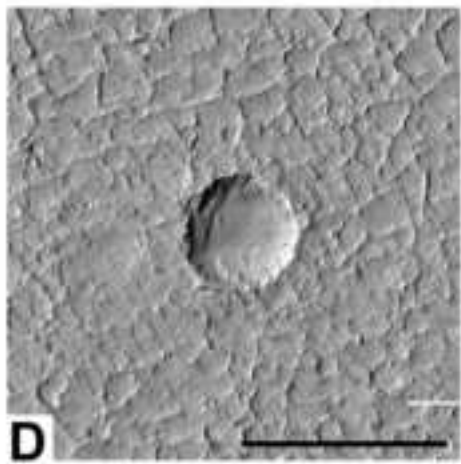
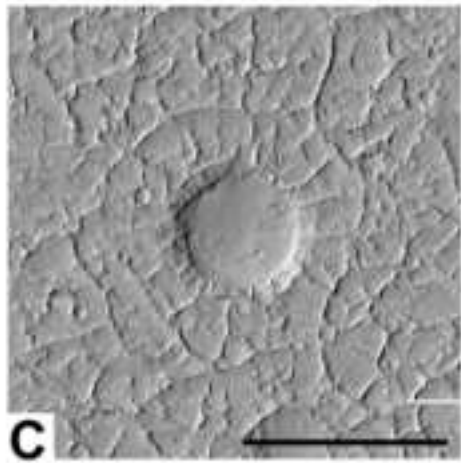
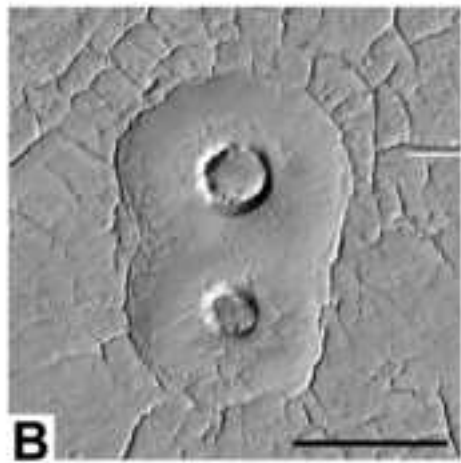
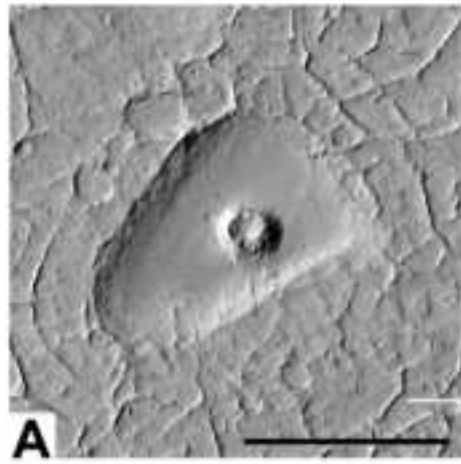




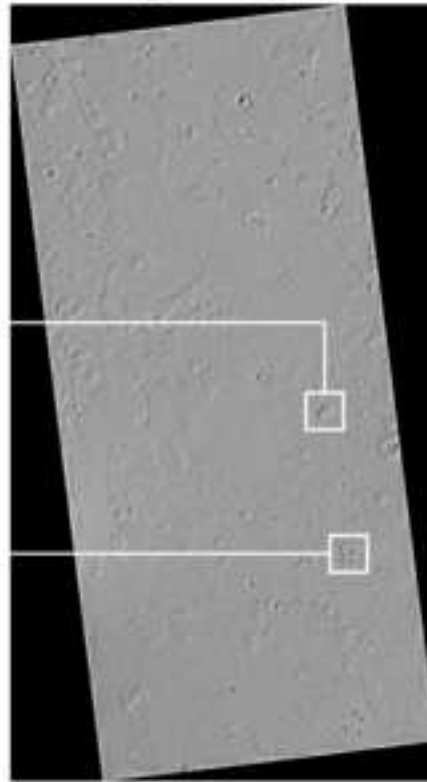




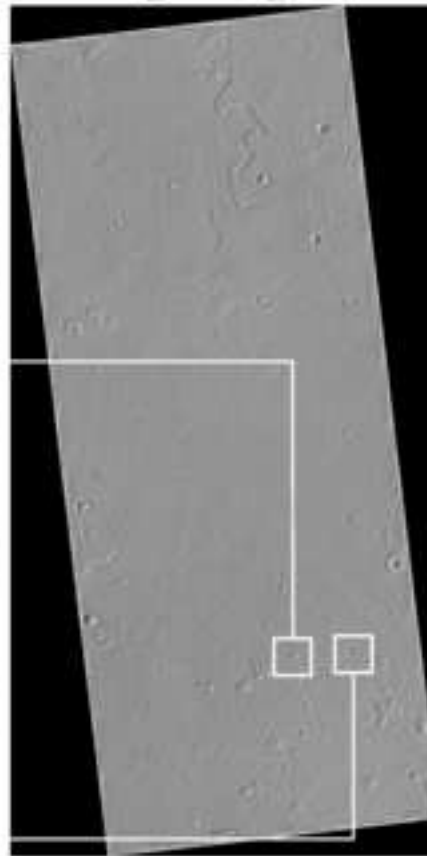




PSP_008382_1980



PSP_008092_1980



ACCEPTED MANUSCRIPT

ACCEPTED MANUSCRIPT